ABSTRACT

BAEK, SEUNGHUN. Design Considerations of High Voltage and High Frequency Transformer for Solid State Transformer Application. (Under the direction of Dr. Subhashish Bhattacharya).

The Solid State Transformer (SST) is one of the key elements proposed by Future Renewable Electric Energy Delivery and Management (FREEDM) Systems Center established in 2008. The main goal of the SST is enable a flexible, controllable and bidirectional power electronics interface for loads, Distributed Renewable Energy Resources (DRERs) [PV, Fuel-cells, Microturbines] and Distributed Energy Storage Devices (DESDs) [Batteries, PHEVs–Plug-in Hybrid Electric Vehicles] to the existing 12kV power distribution grid. The SST will allow reduction of size and weight by replacing bulky conventional transformers at frequency 60 Hz with the multi-stage converters which utilizes high frequency transformer. Operation in high frequency simply makes the transformer compact and light, but there exist many other restraints as well for the high voltage application like dry-type 12kV SST. Additionally, the leakage inductances of the transformer in a soft switching dual active bridge (DAB) dc-dc converter play an important role as an element to determine the amount of transfer power; therefore comprehensive electromagnetic analysis is necessary to optimize the system. This thesis examines entire design procedure and electromagnetic analysis of transformers at operating frequency of 3kHz for a DAB dc-dc converter with insulation to support high voltage and also covers prospective design at operating frequency of 20kHz with another structure eventually targeted with development of high voltage and high frequency capability devices. Three different case studies are

conducted and compared to find the best fit for this specific application and the pros and cons are discussed at the end. Simulation result of Finite Element Method (FEM) and experiment results are provided to confirm the validity and availability of the proposed designs.

Design Considerations of High Voltage and High Frequency Transformer for Solid State Transformer Application

by
Seunghun Baek

A thesis submitted to the Graduate Faculty of
North Carolina State University
in partial fulfillment of the
requirements for the degree of
Master of Science

Electrical Engineering

Raleigh, North Carolina

2009

APPROVED BY:

_____	_____
Dr. Subhashish Bhattacharya Committee Chair	Dr. Alex Huang
_____	
Dr. Mesut Baran	

ACKNOWLEDGMENTS

First and the foremost, I would like to thank my advisor, Dr. Subhashish Bhattacharya. Dr. Bhattacharya led me to study MS program at North Carolina State University and presented me this great opportunity to work in FREEDM Center. I could have courage and will to study in this area thanks to his enthusiasm, knowledge and especially generous advice and care to students in and out. I would not have done this work without him.

I would also like to thank committee members Dr. Alex Q. Huang and Dr. Baran for their valuable lectures and support. Their teaching and knowledge have been always the best source to overcome obstacles and precede my research.

I want to express my gratitude to all the members in SPEC, especially, Jaesung Jung, Jeesung Jung, Jinseok Park, Sungkeun Lim, Woongje Sung who care me like a family and Yu Du who has been helping me with academic advice.

I also very grateful to my friends, Hyoungtae Cho, Jaesuk Lee, Jongmin Lim and Young Cho who have been a good friend since we met in Chicago and Mamiko Arai.

Most importantly, I can never exaggerate my gratitude to my family in Korea, father, mother and elder brother and sister in law who became a member of our family and my lovely niece.

Thank you very much and I love you all.

TABLE OF CONTENTS

LIST OF TABLES

LIST OF FIGURES

CHAPTER 1

1 INTRODUCTION

The design of high frequency transformer under high voltage condition requires more accurate electromagnetic analysis and concern from the control point of view and insulation point as well. High frequency transformers at the DC-DC stage in solid state transformer play an important role for the performance and overall efficiency of SST system, so it is important to select right materials and optimize the design to fulfill all requirements in the operating condition by theoretical analysis and simulation. Even though the high operating frequency makes the transformer compact, there are many restraints which have to be considered, such as insulation, power loss and cost as well. Two different types of winding are considered for Gen-1 SST transformer at operating frequencies of 3 kHz and another one for operating frequency 20 kHz are designed for prospective future SST transformer eventually targeted. Typical solenoidal winding type with Meglas C-Core made of amorphous alloy is selected for operating frequency of 3kHz because the performance of amorphous alloy core is good enough at the given operating frequency with low cost. On the other hand, supreme performance is necessarily required for high operating frequency over 20kHz, hence coaxial winding type with Nanocrystalline toroidal cores is selected. Coaxial transformer has different structure from the conventional solenoidal transformer, so the detail analysis is covered in Chapter 5. The challenge in this work is that how to trade off the pros and cons of the each transformer under the given condition in addition to the high voltage insulation issues to support up to 11,400 VAC without partial discharge or breakdown of the

air because this high frequency transformer is designed as dry-type for environmental and safety issues. This thesis examines mainly efficiency of high frequency transformer depending on the operating condition, wire and core selection and electromagnetic analysis to have a required magnetizing and leakage inductance for the DAB dc-dc converter. The summary of the designs and comparison is in chapter 9 and this thesis is rounded off with the recommendations for future work.

CHAPTER 2

2 SOLID STATE TRANSFORMER TOPOLOGIES AND REQUIREMENTS FOR HIGH FREQEUNCY TRANSFORMER

2.1 Solid State Transformer Topology and operating principle

The SST basically converts the voltage from AC to AC for step-up or step-down with the function same as the conventional transformer. However, the traditional 60 Hz transformer is replaced by a high frequency transformer which is the key to achieve size and weight reduction and the power quality improvement. The solid state transformer consists of three stages, AC/DC rectifiers, a soft-switching Dual Active Bridge converter with a high frequency transformer and a DC/AC inverter.

The basic configuration of a proposed 20 kVA SST interfaced to 12 kV distribution voltage with center-tapped 120V single-phase output is shown in Fig 1. The SST is rated as single phase input voltage 7.2kV, 60 Hz, output voltage 240/120 V, 60 Hz, 1 phase/3 wires. The SST consists of a cascaded high voltage high frequency AC/DC rectifier that converts 60Hz, 7.2 kV AC to three 3.8 kV DC buses, three high voltage high frequency DC-DC converters that convert 3.8 kV to 400V DC bus and a voltage source inverter (VSI) that inverts 400V DC to 60 Hz, 240/120 V, 1 phase/3 wires. The switching devices in high voltage H-bridge and low voltage H-bridges in Fig.1 are 6.5kV silicon IGBT and 600V

silicon IGBT respectively. The switching frequency of the high voltage silicon IGBT devices is 3 kHz, and the low voltage IGBT in the VSI switches at 10 kHz. The 20 kVA SST unit is envisioned as a building block of IEM and also for construction of a larger rated SST. The switching device for high voltage side is a newly packaged 6.5kV 25A H-bridge IGBT module as Fig.1 shows, While for the low voltage side, commercially available 600V/1200V IGBTs are used.

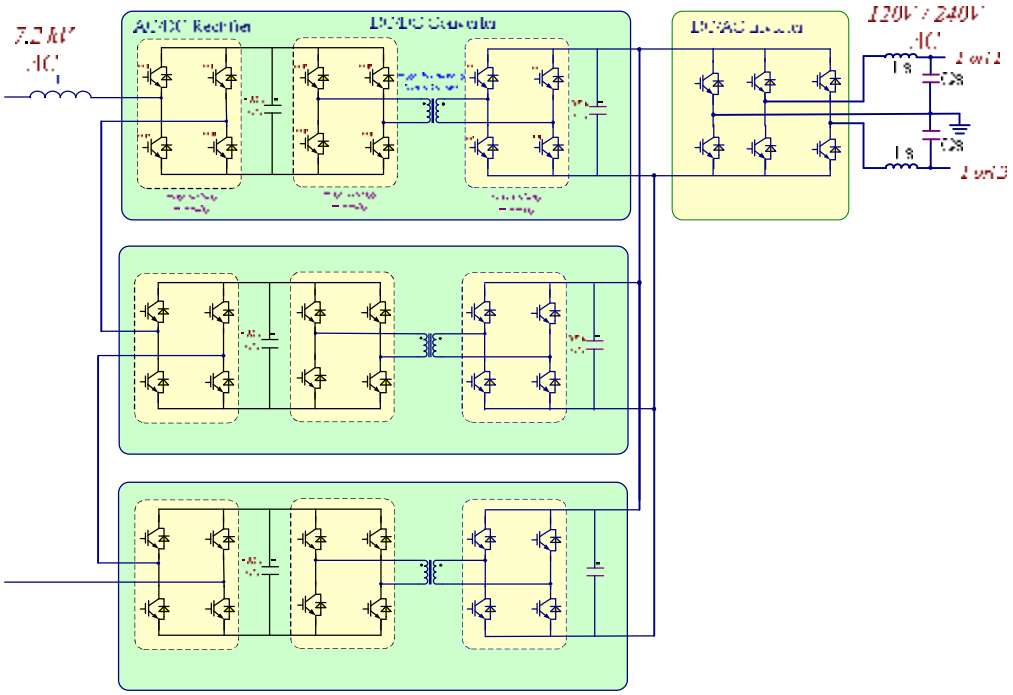

Figure 1 Topology of Gen-1 Solid State Transformer

Fig.2 shows the Gen-2 SST transformer which is consist of only one stage in AC-AC converter. The frequency and power capability range of devices simply indicate the development of power electronics converter in Fig.3. Silicon base devices are placed around

10^9 W-Hz, so Gen-1 SST is almost at the edge of the silicon-based devices. Therefore, Gen-2 SST with one stage can be realized with development of new devices which has high voltage, high frequency and high temperature operation capability, such as possibly SiC devices. The Gen-2 SST must be support three times more power capability which comes with size increase, therefore, the increasing operating frequency is necessary to reduce the size which must come with more accurate and profound AC analysis, such as eddy current, for this application.

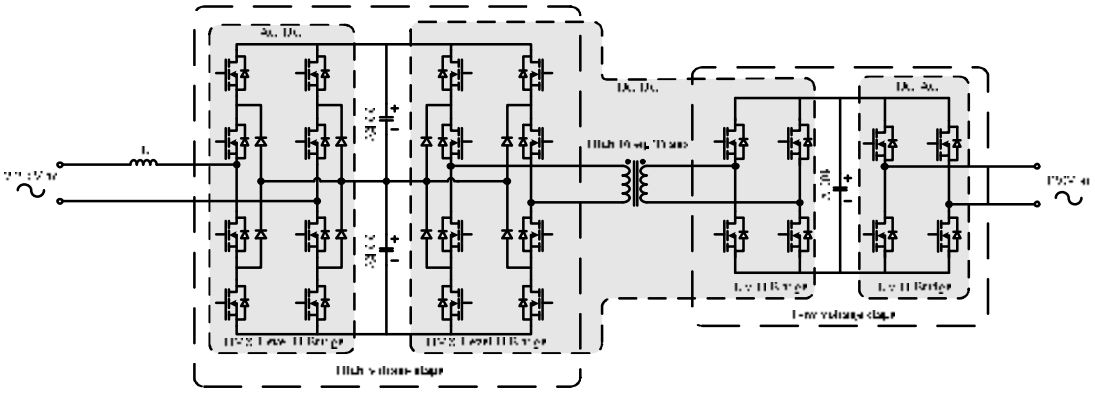

Figure 2 Topology of Gen-2 Solid State Transformer

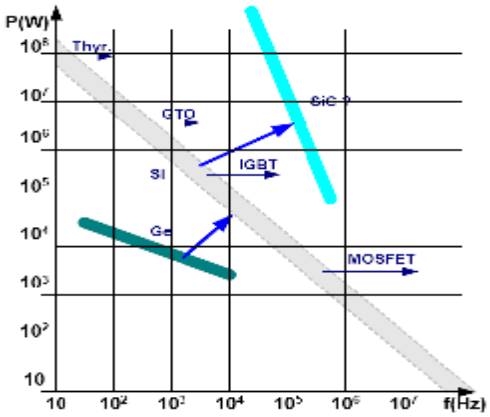

Figure 3 Status of the P*f(W*Hz) of power electronics converters based on different semiconductor materials (Wei Shen, "Design of High Density Transformers for High Frequency High power Converter")

The dual active bridge (DAB) converter which is used for SST high frequency transformer has attractive characteristics for high power and high frequency applications, such as low device stress, no extra reactive component using the leakage inductance of transformer as the main energy transfer element. DAB converter consists of two active bridges connected though the transformer and the amount of power from one DC source to the other is determined by the phase shift between two active bridges Fig. 2.

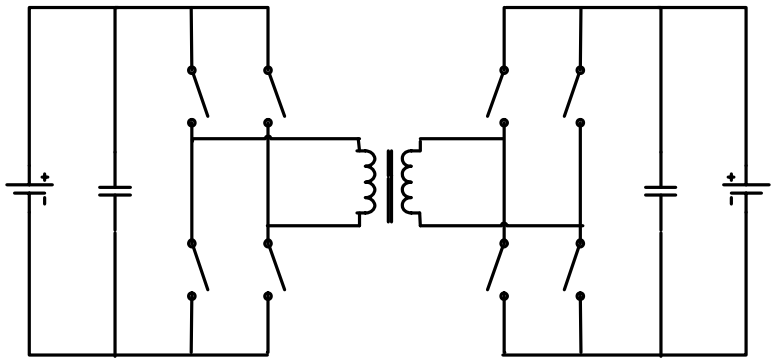

Figure 4 Schematic of single-phase dual active bridge (DAB) converter

The flux density can be obtained by integrating the induced voltage on the winding (2.1.1) and the magnetic field intensity is calculated from the magnetizing inductance (2.2.2). Thereafter, B-H curve is drawn based on data calculated from the equations. The hysteresis loop caused by permanent magnet from a material that stays magnetized is not taken into

account in this curve. The parameters used for this graph is real values of Design-2 separate winding transformer which will be introduced later on.

$$B = \frac{\int v(t) \cdot dt}{n \cdot A_c} \tag{2.1.1}$$

$$H = \frac{n \cdot i(t)}{MPL} \tag{2.1.2}$$

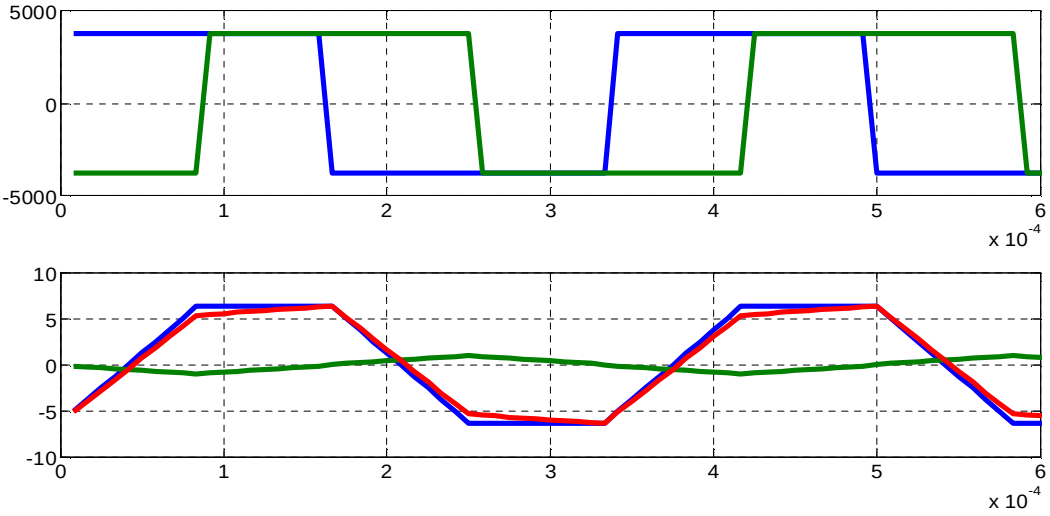

Figure 5 DAB converter voltage and current waveforms
(Top : Primary voltage(blue), Secondary voltage(Green), Bottom: Primary current(red), Magnetizing current(green), Leakage current(blue))
- 3 kHz, phase shift : pi/4, magnetizing inductance :330mH, Leakage inductance : 50mH, Design-1 separate winding transformer

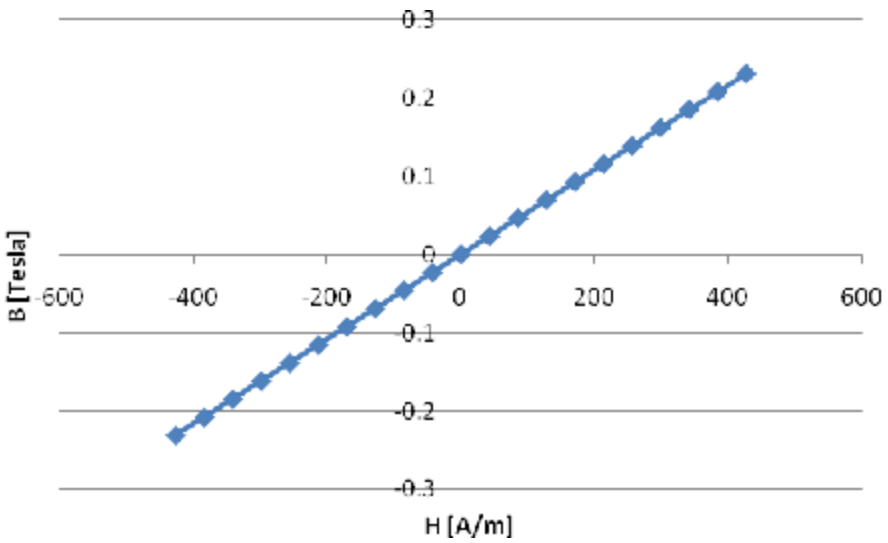

Figure 6 B-H curve (Design-1 separate winding transformer)

The principle of the DAB converter is simple. Two active bridges are connected by high frequency transformer and the phase shift between two bridges determines the amount of power from one DC source to the other. This circuit works at the fixed frequency and square wave mode of operation. The waveform of primary and secondary voltage and current are illustrated in Fig.4. Assuming the input and output voltage are the same as required, the output power is ideally transferred with infinite magnetizing inductance by (2.1.3). V is input and output DC voltage, f is the phase shift between input and output bridges.

$$P = \frac{V^2}{2pf \cdot L} \cdot f \cdot (1 - \frac{|f|}{p}) \qquad (2.1.3)$$

2.2 Required Leakage Inductance with respect to Operating Frequency

Leakage inductance in dual active Bridge converter is a key element to determine the amount of energy transfer. The power transferred from primary to secondary can be represented by (2.2.1). The required leakage inductance with respect to switching frequency of dual active bridge converter is shown in fig 6. The required leakage inductance can be calculated by (2.2.1) in the range approximately from 45.1 to 75.7 mH at 3kHz and from 6.7 to 11.4 mH at 20kHz respectively. Additional external inductor might be required in case of lack of leakage inductance in transformer. This external inductor can lead another volume and structure, so it also needs to be taken care of well. How to deal with this leakage inductance and external inductor for optimization is the key point of the high-frequency high-voltage SST transformer.

$$L = \frac{V^2}{2pf \cdot P} \cdot f \cdot (1 - \frac{f}{p}) \qquad (2.2.1)$$

	High Voltage Side	Low Voltage Side
DC-bus [V]	3800	400
Current at maximal load [A]	2.66	25.27
Power [W]	7kW	
Turns ratio	9.5:1	
Switching frequency [kHz]	3kHz, 20kHz	
Phase Shift	p / 6 ~ p / 4	

Table 1 Specification of Gen-1 SST Transformer

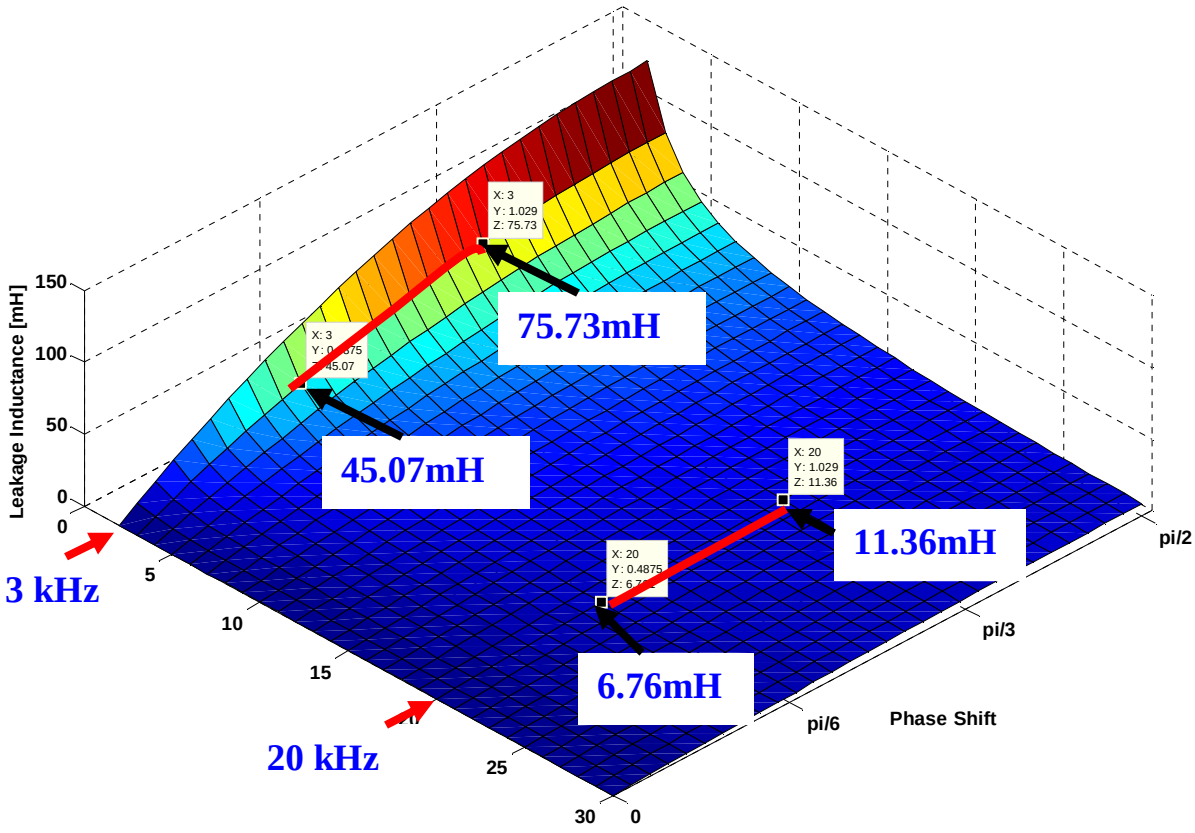

Figure 7 Required leakage inductance with respect to operating frequency and phase shift for DAB converter

CHAPTER 3

3 CORE MATERIAL AND STRUCTURE SELECTION

3.1 Core Material Comparison

One of the basic steps in transformer design is the selection of proper core material. Selecting suitable core material for particular applications is important to design transformers. A material easily magnetized and demagnetized, referred to as 'soft magnetic material', is generally used for high frequency transformers. There are several typical materials of soft magnetic which can be considered for the high frequency transformer in solid state transformer based on the specification proposed. Even though ferrite cores are most popularly used for high frequency applications, the ferrite material has very low saturation flux density around 0.3-0.5 T which makes the transformer bulky especially for high voltage applications, hence ferrite core is left out as core material in this paper. The main factor to select the core material is core losses for different frequencies over flux density change.

3.1.1 **Silicon Steel**

Silicon steel is one of the most popular materials for use in soft magnetic applications. They have high saturation flux density (>1.5T) and good permeability. As long as the frequency is low, laminations with 10 mil or higher thickness offers excellent performance with low cost. For higher frequency from 400Hz to 10kHz, the lamination thickness should

be further decreased due to excessive eddy current loss. Some manufactures provide silicon steel laminations with gauge down to 1mil, which are suited for high frequency applications. However, compared with nanocrystalline and amorphous core materials, its specific loss is still very high.

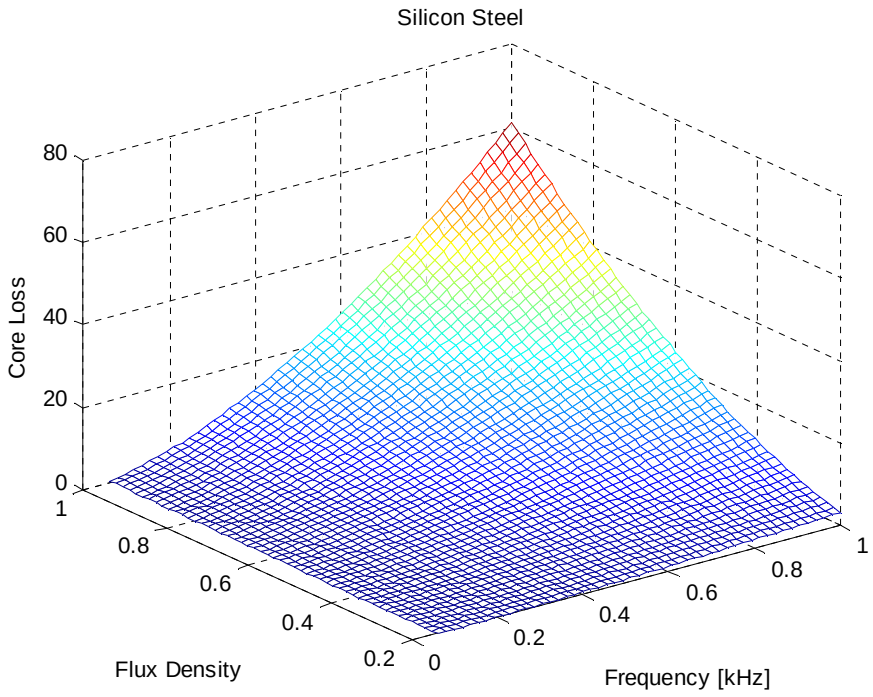

Figure 8 Core loss per kg in terms of frequency and flux density of Silicon Steel (Thickness 14 mil)

3.1.2 **Amorphous Alloy**

The second candidate is amorphous alloy core. In contrast to typical crystalline metals which have a highly ordered arrangement of atoms, amorphous alloy, known as Metglas, are non-crystalline. Metglas-2605 is composed of 80% iron and 20% boron. Amorphous alloy material has not only high permeability like a ferrite but also high saturation flux density up to 1.56T. Ferrites is also good material for high frequency transformer because of the low core loss but the saturation flux density is around 0.3~0.5 Tesla which requires more cross sectional area of cores. Basically, high saturation density allows small size of the core as long as the core loss and temperature rise requirement is fulfilled. Powerlite c-core made of iron-based Metglas amorphous alloy is laminated with typical lamination thickness of 1mil. The specific core loss can be several times lower than silicon steel even though it is still higher than that of nanocrystalline cores. Nonetheless, the cost of amorphous alloy core is much lower than nanocrystalline and the performance/cost factor is excellent in terms of the frequency range of 1~3 kHz. In addition, large geometry are commercially available, which provide great design flexibilities and a thin air gap can be added to prevent core saturation due to DC bias current from dual active bridges. According to the Fig. 9, we can see that the core loss is fairly low in range between 1~3 kHz, approximately under 20W/kg as long as the flux density is not over 1.0 T. Amorphous alloy cores shows good enough performance at given requirement and cost effective too, therefore Metglas powerlite c-cores are employed to design the 3kHz high frequency transformer of solid state transformer on condition that the flux density is less than 1.0T.

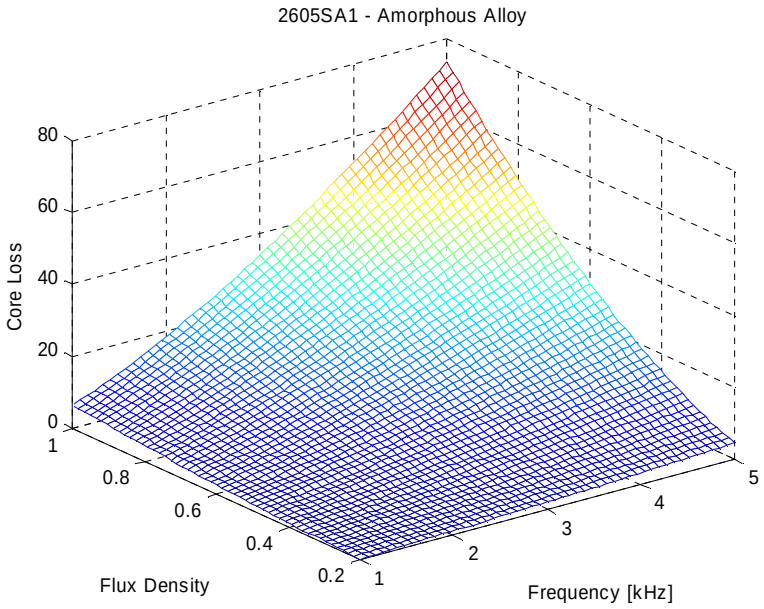

Figure 9 Core loss per kg in terms of frequency and flux density of 2605SA1

3.1.3 **Nanocrystalline**

The third one is nanocrystalline cores. Nanocrystalline cores are generally metallic tape-wound cores made of nanocrystalline soft magnetic material. They exhibit high saturation flux density, typically higher than 1.0 Tesla and extremely low specific losses, compared with silicon steel, amorphous and ferrite cores in the frequency range up to several tens of kilo hertz. This can result in a low volume and weight transformer design. Copper losses can be kept small by users due to the large usable induction swing and high permeability, for example, the number of turns can be small. Although special shapes in oval or rectangular design with or without cut can be produced, the standard off-the-shelf core

shape for nanocrystalline cores is toroidal uncut tape-wound cores. The leakage inductance is small due to the toroidal geometry and low number of turns possible. The preliminary design based nanocrystalline core indicates extremely high core cost for SST transformer. On the other hand, insulation issue is difficult for toroidal cores. Also the largest geometry of commercially available nanocrystalline cores does not provide sufficient window area for 3kHz operating frequency. Despite the high cost, high quality performance of nanocrystalline is necessarily required for 20kHz operating frequency Fig.10.

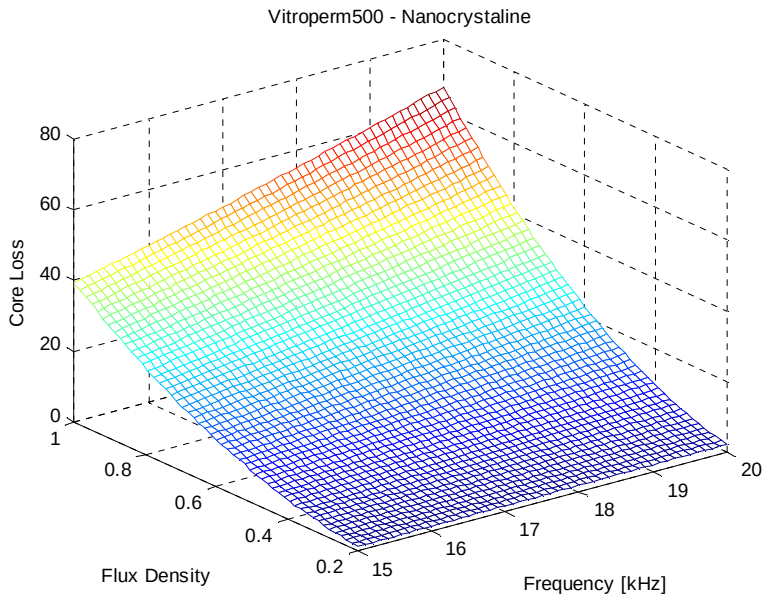

Figure 10 Core loss per kg in terms of frequency and flux density of Vitroperm500

3.2 Core Selection for Operating Frequency of 3kHz

The power handling capability of a core is related to the product of winding area (Wa) and cross-sectional area (Ac), which is called area product (). Even though additional care is required for high voltage application, it is enough to help us to initially choose magnetic cores for given specification of design. Another main concern of designing transformer at 3kHz is possibly eliminating external inductors to make up the lack of leakage inductance in transformer. External inductances are going to be almost a half as big as transformer at 3kHz, so it makes the system bulky and complex and also require another structure. In case of operating frequency 3kHz, it is very likely to eliminate the external inductors with only leakage inductance in transformer, so we will investigate step by step in Chapter 3 and 4 to figure out the best fit for Gen-1 SST high frequency transformer without external inductors.

Supposed that $J_{\max} = 200A/cm^2$, $K_u = 0.1$, $K_f = 4.0(square\ wave)$ are given for Gen-1 SST high frequency transformer, the required minimum area product is approximately $1900cm^4$, (3.2.1). As expected to be seen in chapter 4, the bigger the ratio of 'c' and 'b', the larger leakage inductance the transformer has. Considering the insulation requirement under high voltage and the larger leakage inductance to eliminate or reduce external inductors at the switching frequency 3khz, 2 or 3 pairs of AMCC1000 cores (Ap of a pair of AMCC1000= $966\,cm^2$) are chosen to be used with margin, Table 2.

$$A_p = \frac{(P_{in} + P_{out}) \cdot 10^4}{B_{ac} \cdot f \cdot J \cdot K_f \cdot K_u} \tag{3.2.1}$$

Core Dimension [mm]						Performance parameters				
A	b	c	d	e	f	Lm[cm]	Ac[cm^2]	Wa[cm^2]	Ap[cm^4]	Mass[g]
33.0	40.0	105.0	85.0	106.0	171.0	42.7	23.0	42.0	966.0	7109

Table 2 Dimension of AMCC1000 Powerlite C-core

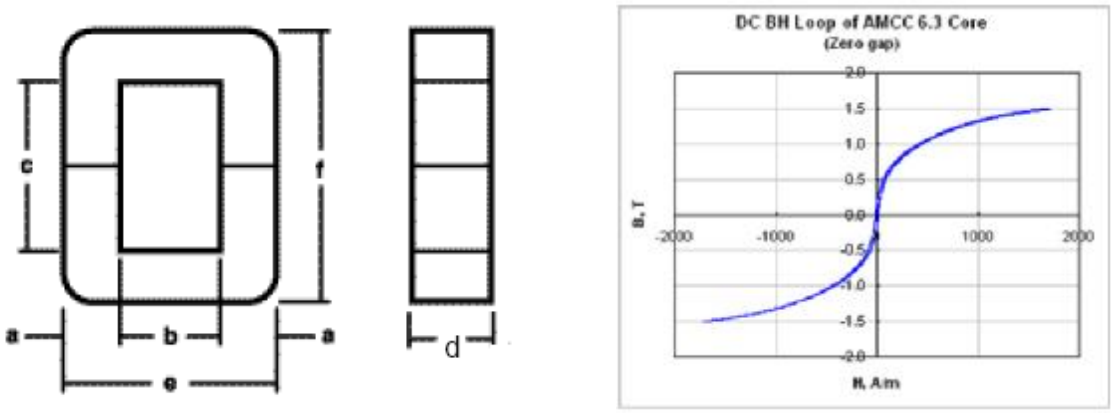

Figure 11 Geometry of Metglas AMCC C-Core (left) and the BH curve (right)

3.3 Core Selection for Operating Frequency of 20kHz

The transformer type for 10kHz application is decided to use coaxial winding transformer type. There are many advantages of coaxial winding transformer, even though we have considerable physical restriction for our application under high voltage and low current. The primary windings are conducting tube forms in window area of toroidal cores, so there is mechanical restriction of the number of turns. Therefore, the size of the transformer needs to be overkill in terms of power capacity to reduce the number of turns.

Nonetheless, there are also many advantages of the coaxial winding transformer. Most importantly, the most parameters, such as inductance, capacitance and power loss, are easily and fairly accurately predicted by calculation. In the dual active bridge application, these parameters play a significant roles, so this very desirable feature of coaxial winding transformer. The same parameters ($J_{\max} = 200A/cm^2$, $K_u = 0.2$, $K_f = 4.0(square\ wave)$, $B_{ac} = 0.77$) are used for 10kHz application. 12 of Vitroperm T64004-W908 are used.

Core dimension Dout*dn*h [mm]	Cross sectional area [em^2]	Mean path length [cm]	Part number
80*63*20	1.24	22.5	4-L2080-W722

Table 3 Dimension of Vitroperm

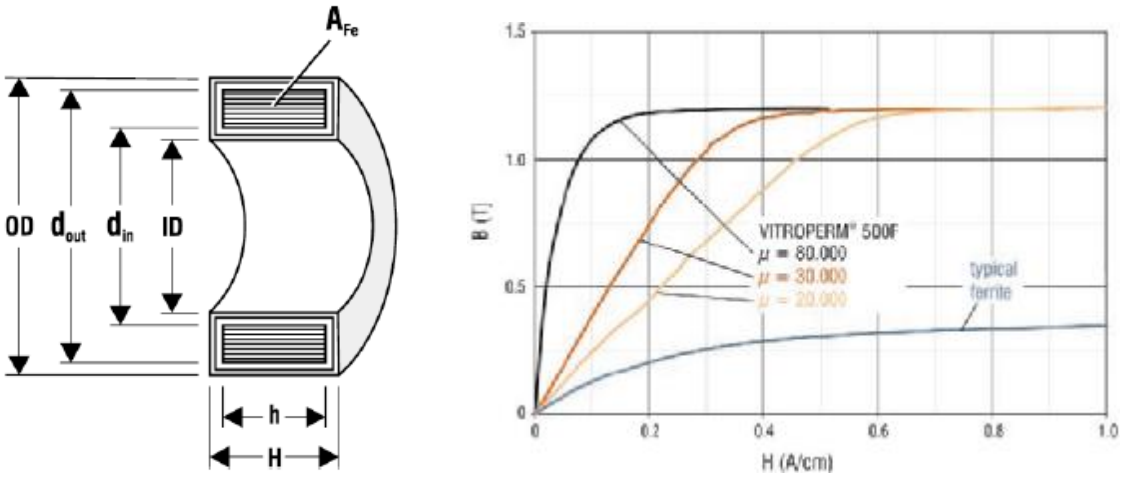

Figure 12 Geometry of Vitroperm 500 (left) and the BH curve (right)

3.4 Wire Selection

The required cross-sectional area of the winding on high voltage side is $0.0110 cm^2$ (diameter : 0.1183cm) and the cross-sectional area of the winding on low voltage side is $0.105 cm^2$ (diameter : 0.3656cm) to have the current density of $200 A/cm^2$. The skin depth at the frequency of 3kHz is 0.1378cm, (3.4.1). The recommended strands wire gauge at frequency of 1kHz~10kHz is around 30AWG and the insulation to support 3.8kV AC is required, so the PFA: high voltage wire AWG17 (35/32) and 350/32 Litz wired from New England Wire are chosen for high-voltage and low-voltage side respectively. Table 4 shows the specification of the windings.

$$skin\ depth\ @100°C \quad e = \frac{K_1}{\sqrt{f(kHz)}}(um) \qquad K_1 = 2385\ @\ 100°C \tag{3.4.1}$$

High Voltage Side	Current density	$200\ A/cm^2$
	Required copper area	$0.0110\ cm^2$ (dia 0.1183cm)
	Wire Gauge	35/32
	Diameter of Single strands	0.0202cm
	Insulation	PFA insulation (0.0135"=0.0343cm)
	External Diameter and cross-sectional area without wrapping	0.06"=0.1524cm, $0.0182\ cm^2$
	Finished wire diameter	0.087"= 0.221cm
	DC resistance	$173.8 u\Omega / cm$ (20 C)
Low Voltage Side	Current density	$200\ A/cm^2$
	Required copper area	$0.105\ cm^2$ (dia 0.3656cm)
	Wire Gauge	350/32
	Diameter of Single strands	0.0202cm
	Insulation	PFA insulation (0.02"=0.0508cm)
	External Diameter and cross-sectional area without wrapping	0.203"=0.515cm, $0.208\ cm^2$
	Finished diameter	0.243"=0.617cm
	DC resistance	$15.8 u\Omega / cm$ (20 C)

Table 4 Specification of wires

3.5 Comparison and Selection of Transformer Structure

There have been a lot of researches conducted about different structures and winding methods for power electronics converters to maximize the operating frequency with low power losses and temperature rise. By and large, there are two dual structures, solenoidal and coaxial winding transformers. We are going to investigate the magnetoelectric characteristics of each structure and see what are the pros and cons at different operating frequencies under high voltage and low current condition.

3.5.1 Duality of Solenoidal and Coaxial Winding Transformers

The solenoidal winding structure and coaxial winding structure are the duals of one another. In case of the solenoidal winding structure, the magnetic flux flows parallel to the cylindrical axis and the current encircles the cylindrical axis. On the contrary, the flux encircles the cylindrical axis and the current flows parallel to the cylindrical axis by right hand rule in the case of coaxial winding structure.

Solenoidal winding transformer is the most conventional geometry of transformer. A conductive wire is wrapped around the core so that the electric current within the coil of wire produces magnetic field in the magnetic core. The change of magnetic field induces a

voltage in the other coil of wire on the magnetic core by Faraday's law. The equivalent circuit is represented below in Fig. 15. Leakage flux density is on the both side and divided almost equally. Even though the method to calculate the leakage inductance of conventional transformer has been studied for long time, there are numerous factors to affect the leakage inductance, such as geometry and the way of winding. It is predicted by simplification but it is complicated and has a possibility of error.

The coaxial winding transformer simply consists of an outer conducting tube in toroidal core and another winding is placed inside cylindrical outer winding. Assuming the outer winding covers inner winding ideally, the flux density of outer winding entirely links to the inner winding so that outer winding does not have leakage inductance in case of coaxial winding. The equivalent circuit model is represented in Fig.16. Additionally, the cylindrical shape is relatively easy to analyze so the inductances are quite predictable with minor error. Nonetheless, coaxial winding has a restriction of number of turns due to the physical difficulty. The outer winding can be multiple in a couple of ways even though one turn of outer winding is preferable to simplify the geometry and analysis. This is one of the downsides of the coaxial winding transformer because SST high frequency transformer requires high number of turns due to high voltage rating.

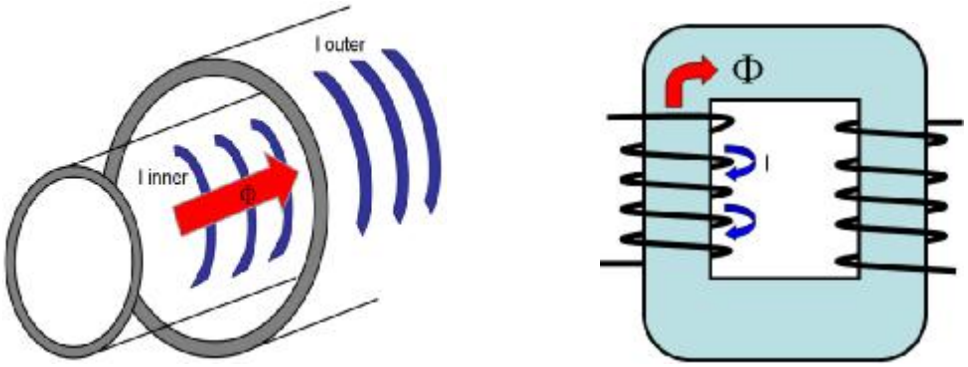

Figure 13 Magnetic flux and current flow in solenoidal winding transformer

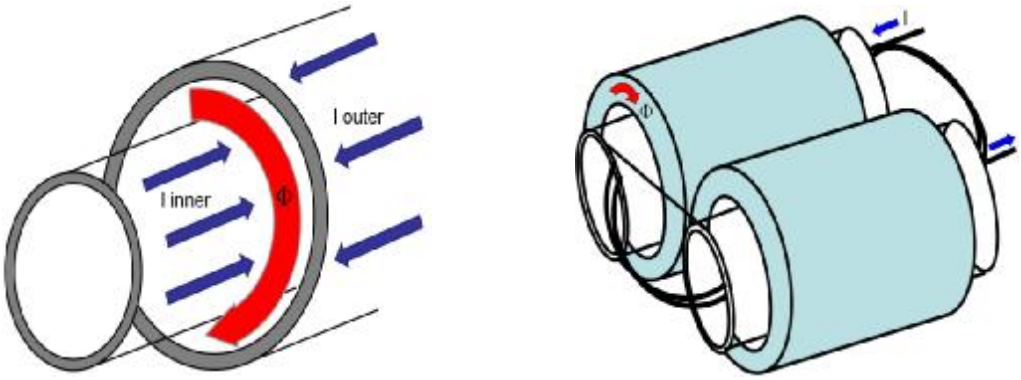

Figure 14 Magnetic flux and current in coaxial winding transformer

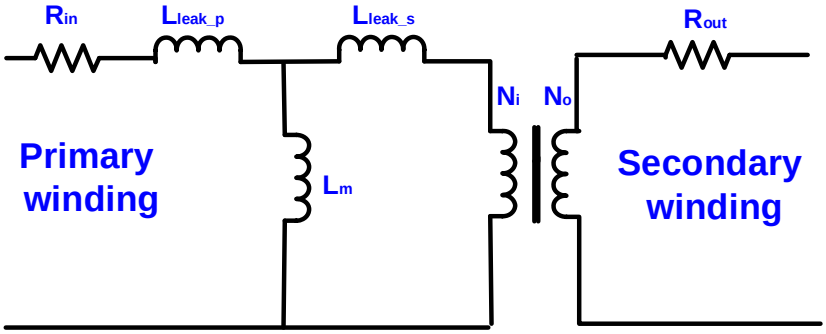

Figure 15 Equivalent circuit for the two winding solenoidal transformer

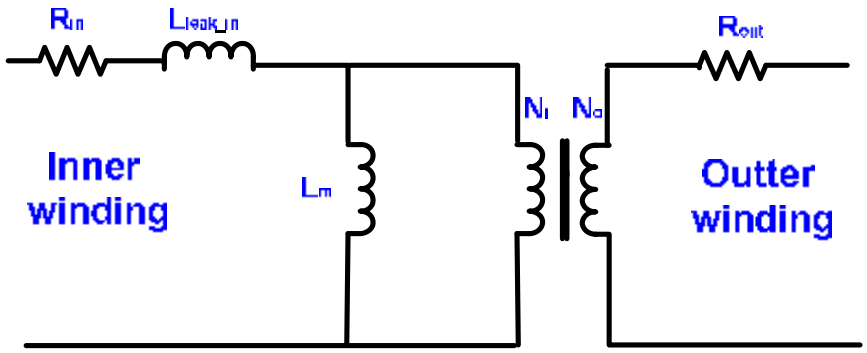

Figure 16 Equivalent circuit for coaxial winding transformer

Generally speaking, it is obvious that a coaxial winding transformer shows better performance even though it is more difficult to build mechanically and expensive. Nonetheless, there are other factors which we also have to take into account for DAB converter to use coaxial winding type. First of all, coaxial geometry has a significant physical restriction of the number of outer winding turns. The outer windings, which are thin tubular copper conductor, of coaxial winding transformer are placed in window area of the toroidal core. The concentric tubular conductors have to be connected in series in safety inside window area in case of multi turn of outer winding. This is mechanically very difficult to build and not good for safety reason as well. There are two ways to reduce the number of turns in low frequency, which are increasing flux density or cross sectional area. Increasing the flux density is limited to avoid core saturation and increasing cross sectional area means larger size. In contrast, conventional solenoidal transformer is easy to build with low cost and has an unexpected additional advantage of high leakage inductance even though

it depends on the method of winding. Solenoidal winding type is more suitable and decided to be used at 3kHz. In case of frequency 20kHz, the leakage inductance is required to be more accurate and predictable for design, so coaxial winding type is decided to be used at 20kHz.

CHAPTER 4

4 LOSS AND ELECTROMAGNETIC ANAYSIS OF SOLENOIDAL WINDING TRANSFORMER DESIGN

4.1 Core Loss

Core loss is one of the most important ac properties of transformers. Some of energy is not recoverable due to the magnetization of core material and transfers to heat. It is observed as hysteresis of the B-H loop. The ac flux in the core induces current proportionally with the excitation frequency, so the core loss increases as the square of the excitation frequency assumed the core material is pure resistive. Amorphous alloy 2605SA1 has its own empirical equation provided by the datasheet in terms of frequency and the flux swing (4.1.1). If we select 0.23 of the optimal Bac value, the core loss per kilogram is 2.647 W/kg and the total of 3 pairs of AMCC1000 is 56.455W.

$$Watt/kg = k \cdot (f/1000)^{(m)} \cdot B_{ac}{}^{(n)} \quad 2605SA1: \; k = 6.5,\; m = 1.51,\; n = 1.74 \tag{4.1.1}$$

Switching frequency [kHz]	3kHz
Bac [T]	0.23
Mass of a pair of AMCC1000 [kg]	7.109
Total mass [kg]	21.327
Core loss per kilogram [W/kg]	2.647
Total core loss [W]	56.455

Table 5 Magnetic flux density and core loss

4.2 Winding Loss

DC winding loss can be easily calculated regardless of the frequency, but AC winding loss in Litz wire is not easily estimated because it is affected by many factors. Various formulas have been derived to achieve accurate AC winding losses in Litz wire. In this paper, we use the application note from 'New England Wire Technology'.

The skin depth at the frequency of 3kHz is 0.1378cm (4.2.1). Recommended wire gauge which can properly eliminate the skin effect at the frequency of 1~10kHz is approximately 30AWG. 32AWG is chosen as wire gauge for strands considering the case of increasing the switching frequency. The ratios of alternating-current resistance to direct-current resistance for an isolated solid round wire (H) in terms of a value (X) are shown in Table 6 and 7.

$$skin\ depth\ \ e = \frac{K_1}{\sqrt{f(kHz)}}\ (um) \quad (K_1 = 2386,\ 100°C) \tag{4.2.1}$$

$$X = 0.271 \cdot D_M \cdot \sqrt{F_{MHz}}\ , \qquad \text{Eddy current basis factor}\ \ G = \left(\frac{D_i \cdot \sqrt{f}}{10.44}\right)^4 \tag{4.2.2}$$

$$\frac{R_{ac}}{R_{dc}} = H + K \cdot \left(\frac{N \cdot D_i}{D_o}\right)^2 \cdot G \tag{4.2.3}$$

F=operating frequency, N=The number of strands in the cable

D_i =Diameter of the individual strands over the copper in inches

D_o =Diameter of the finished cable over the strands in inches

G : Eddy current basis factor F : Operating frequency

N : # of strands in the cable Di : Diameter of individual strands

Do : Diameter of the finished cable K : constant (2 when N>27)

X	0	0.5	0.6	0.7	0.8
H	1.0000	1.0003	1.0007	1.0012	1.0021

Table 6 The value of X for copper wire is determined

N	3	9	27	infinity
K	1.55	1.84	1.92	2

Table 7 Constant depending on N

The current and voltage waveform on primary and secondary side of transformer was shown in a previous chapter. Supposed that the magnetizing inductance is large enough, current waveform can be considered trapezoidal for convenience. The Fourier series method is the most typical way to analyze non-linear load current. The current waveform can be represented in Fourier series form with respect to phase shift (4.2.4). As the harmonic order increases, the magnitude of the corresponding current decreases, only the first few terms of the series are of interest. In this calculation, the quantities at higher than harmonic order of 20 are ignored. For example, the Fourier series quantities are shown in table 7 assuming the inductance is 250mH and the phase shift is pi/3. As you can see in Table 8 and 9, the impact of the skin effect based on the ratio between Rac and Rdc is almost ignorable on the high voltage side. The Rac-Rdc ratio is quite high on low voltage side due to the thick large copper area over 9^{th} order harmonics components but the magnitude is already less 5% of the total current. Therefore, there is no significant effect of frequency at frequency 1kHz.

Fourier Series – odd function

$$b_n = \sum_{n=1}^{\infty} \frac{4 \cdot V}{T \cdot L} \cdot \frac{\sin(\frac{n \cdot p \cdot \Phi}{T}) + \sin(\frac{n \cdot p \cdot (T - \Phi)}{T})}{(\frac{2np}{T})^2} \qquad (f = 1kHz) \tag{4.2.4}$$

$$i(t) = \sum_{n=1}^{\infty} b_n \sin \frac{np}{T/2} t \tag{4.2.5}$$

Harmonic order	Freq [kHz]	I [A]	I rms [A]	Rac/Rdc
1	**1**	3.0802	2.178	1.0005
3	**3**	0.6845	0.4840	1.0049
5	**5**	0.1232	0.0871	1.0135
7	**7**	0.0629	0.0444	1.0265
9	**9**	0.0761	0.0538	1.0438

Table 8 Fourier series quantities and ac resistance on high voltage side (1kHz)

Harmonic order	Freq [kHz]	I [A]	I rms [A]	Rac/Rdc
1	**1**	29.2616	20.6910	1.0057
3	**3**	6.5026	4.5980	1.0511
5	**5**	1.1705	0.8276	1.1418
7	**7**	0.5972	0.4223	1.2779
9	**9**	0.7225	0.5109	1.4595

Table 9 Fourier series quantities and ac resistance on low voltage side (1kHz)

4.3 Inductance Analysis

The transformer is an electrical device on the basis of the concept of magnetic coupling. Two of the key electrical parameters when designing a solid-state transformer

using dual active bridge converter are the magnetizing and leakage inductance. Typically, the low leakage inductance, the better it is for a normal transformer application because high leakage inductance and winding capacitance may cause an undesirable output signal such as phase shift, timing error, noise and overshoot. On the other hand, the leakage inductance in transformer is used as the main energy transfer element in DAB converter. Therefore, the leakage inductance value is not just expected to be small in this case but carefully decided in advance and adjusted by demand for required performance of transformer.

4.3.1 **Magnetic Field Distributions in Core**

We are going to analyze two different types of winding, separate and layered winding. Generally, layered winding is preferable because it has lower leakage inductance than the separate winding does. Nonetheless, we have to see which one will be best fit for DAB converter under the condition quite large leakage inductance is required to transfer energy as one of the main element. As stated beforehand, the external inductor leads structural complex and bulky size. We can possibly have additional benefit from the large leakage inductance in separate winding by carefully designing and utilizing the leakage inductance.

The simplified leakage flux line of core and winding are illustrated fig 17. There is basically relatively large mutual flux in the core. In addition, leakage flux is also present, which doesn't link between two windings due to the symmetrical structure. The leakage flux flows vertically in window area. The magnetic motive force in core is negligible due to high

permeability, so we can assume total MMF is in window area. The geometry of winding can be simplified by converting the round wire to the square wire. The thickness of the square wire is derived by make the same effective copper area of square wire to round wire (4.3.1.1).

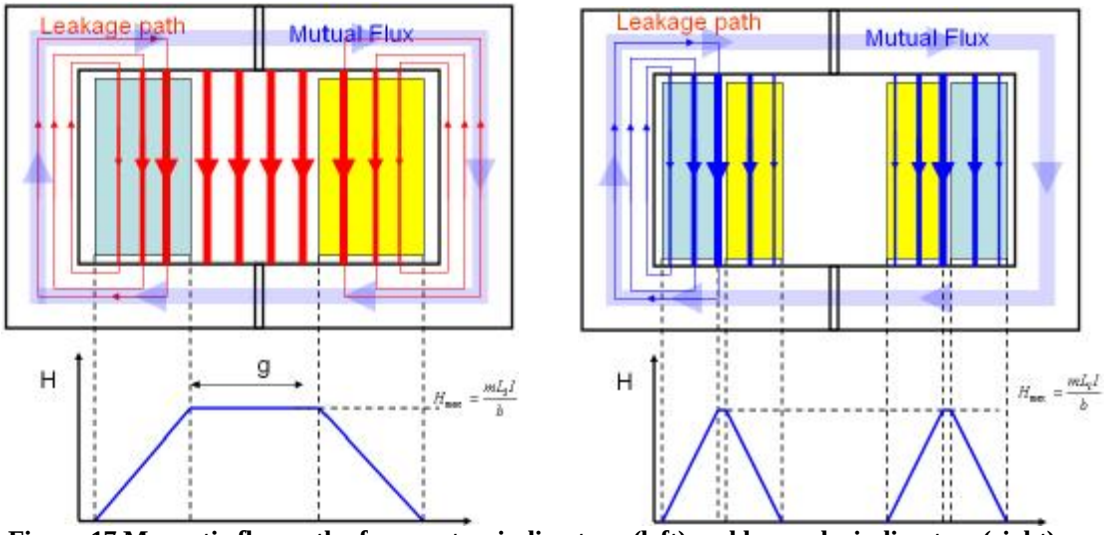

Figure 17 Magnetic flux path of separate winding type (left) and layered winding type(right)

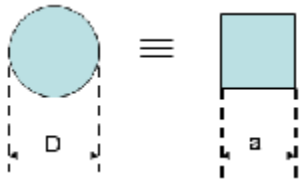

Figure 18 Conversion from circular wire to square wire

$$\frac{pD^2}{4} = a^2, \quad a = D\frac{\sqrt{p}}{2} \tag{4.3.1.1}$$

4.3.2 **Magnetizing Inductance Analysis**

When two inductors (coils) are closely located closely, the magnetic flux caused by current in one coil links with the other coil. This phenomenon is called 'mutual inductance'. The inductance relates the voltage induced in the same coil is called 'self inductance'. The magnetizing inductance can be represented by the mutual inductance times square of the number of turns. The magnetomotive force MMF between two points x1 and x2 is represented by (4.3.2.1). dl is a vector length pointing in direction of the path. Assuming there is an uniform strength of the magnetic field, the magnetizing force can be simplified $F = H \cdot l_m = n \cdot i$ by Ampere's law. The total magnetic flux Φ through a surface S having area A_c is represented by (4.3.2.2) and it can be simplified assuming flux density is normal to the surface $\Phi = B \cdot A_c$. The winding current works as sources of MMF and the average flux flows inside the core. The length of the closed path where the flux flow is called mean magnetic path length l_m. Since assuming that the magnetic field strength is uniform, the induced voltage caused by the flux is given by (4.3.2.3) according to Faraday's law, and the inductance considering airgap can be obtained (4.3.2.4) by magnetic circuit method. The core material permeability m is expressed as the product of the relative permeability m_r and m_0. Even thought the air gap decreases the inductance, we can adjust the inductance value with the thickness of airgap and it allows higher values of current without saturation. Transformer designer also have to keep it mind that there is not exact standard unit for magnetic and be familiar with manipulation and conversion of unit, Table10.

$$F = \int_{x_1}^{x_2} H \cdot dl \tag{4.3.2.1}$$

$$\Phi = \int_{A_c} B \cdot A_c \tag{4.3.2.2}$$

$$v(t) = nv_{turn}(t) = n\frac{d\Phi(t)}{dt} = n \cdot A_c \frac{dB(t)}{dt} = m \cdot nA_c \frac{dH(t)}{dt} = \frac{m \cdot n^2 A_c}{l_m}\frac{di(t)}{dt} \tag{4.3.2.3}$$

$$L_M = \frac{n_1^2}{\frac{l_c}{m \cdot A_c} + \frac{l_g}{m_0 \cdot A_c}} \tag{4.3.2.4}$$

Quantity	MKS	cgs	Conversions
Core material equation	$B = m_r m_0 H$	$B = m_r H$	
B	Tesla	Gauss	1 T=10^4 G
H	Ampere/meter	Oersted	1A/m=4*pi*10^-3 Oe
Φ	Weber	Maxwell	1Wb=10^8Mx, 1T=1Wb/m^2

Table 10 Conversion of standard units in magnetic

The calculation is conducted with assumption that there is no leakage inductance. Typically, leakage inductance is relatively small to the magnetizing inductance, so it was ignored in this calculation. Table 11 shows the results of simulation and calculation. We are going to see the comparison of these results and experimental data later in chapter 7.

Airgap Thickness{mm}	0.055	0.127	0.191	0.267	0.33	0.406	0.508	0.559	0.635	0.72
Calcualation [mH]	23.438	16.893	13.533	10.948	9.451	8.113	6.818	6.314	5.687	5.119
Simulation Separate winding[mH]	22.563	16.878	13.986	11.975	10.334	9.088	7.838	7.114	6.807	6.027
Simulation Layered winding[mH]	22.408	16.851	13.933	11.628	10.291	9.079	7.887	7.422	6.840	6.307

Table 11 Comparison of magnetizing inductance between calculation and simulation result with AMCC250

4.3.3 **Leakage Inductance Analysis with Separate Winding**

There is a leaking flux which does not magnetically couple between in magnetically coupled circuit. This leaking flux alternately store and discharge magnetic energy so works as an inductor in series in the circuit. This can cause the voltage drop across the reactance, hence it result in poorer supply regulation in typical applications. The leakage inductance plays an important role in DAB converter because it is one of elements to control amount of power.

Assumption

1. Square section conductor has the same section of circular ones
2. Leakage flux in core is ignored.
3. Uniform and symmetric magnetic field in the core window
4. Current density is constant and the magnetic field varies linearly

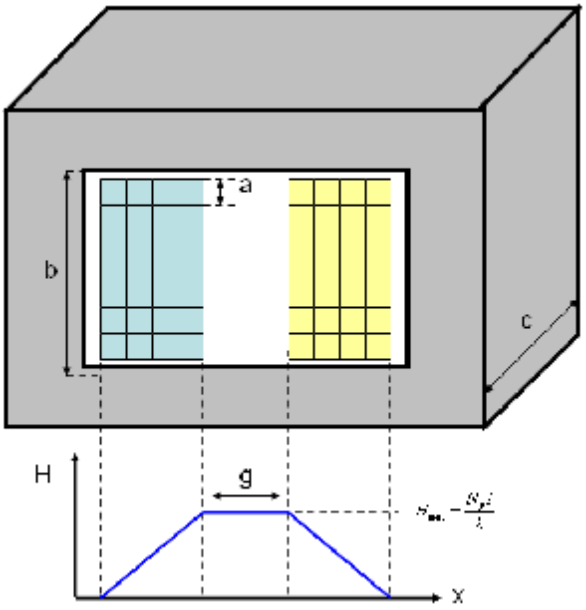

Figure 19 Simplified magnetic field distribution in window area

The stored energy in magnetic field is obtained by (4.3.3.1) and the maximum magnetic field density and the magnetic field intensity in winding with DC current I are represented by (4.3.3.2). Therefore, inductance in a certain volume with the maximum constant magnetic field intensity is represented (4.3.3.4) and the winding is represented by (4.3.3.5). In the case of solenoidal separate winding transformer ,

Leakage inductance of C-C core transformer can be represented by

$$W = \frac{1}{2}LI^2 = \frac{1}{2}m_0 \oint_V H^2 dV = \frac{1}{2}m_0 H^2 V \text{ (Constant magnetic field)} \qquad (4.3.3.1)$$

$$H_{\max} = \frac{N_p I}{b} \tag{4.3.3.2}$$

$$H(x) = \frac{N_p I}{a \cdot b \cdot m} x \tag{4.3.3.3}$$

$$L = \frac{m_0 \cdot N_p^2 \cdot V}{b^2} \qquad V = b \cdot g \cdot c \tag{4.3.3.4}$$

$$\frac{1}{2} L I^2 = \frac{1}{2} m_0 \cdot b \cdot c \cdot \int_0^{ma} \left(\frac{N_p I}{a \cdot b \cdot m}\right)^2 dx \rightarrow \quad L = \frac{m_0 \cdot c_t \cdot N_p^2 \cdot m \cdot a}{3b} \tag{4.3.3.5}$$

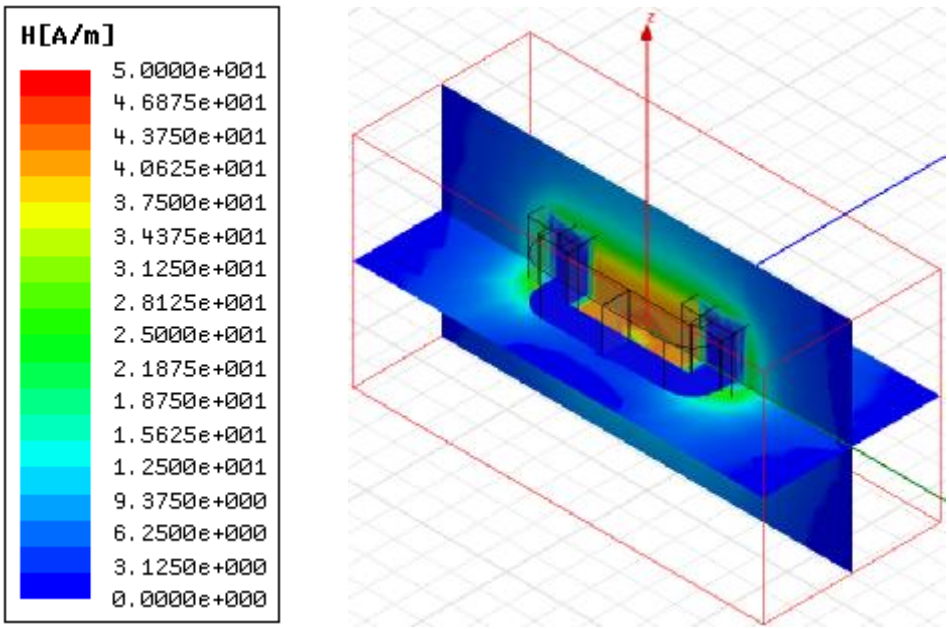

Figure 20 Magnetic field intensity distribution in separate winding with airgap 0.25mm

4.3.4 **Leakage Inductance Analyses with Layered Winding**

In case of layered winding, most energy is stored between the windings, hence, the calculation becomes more obvious and simple. Assuming there is no energy outside windings, the leakage inductance in layered winding is represented (4.3.4.1)

$$L = 2 \cdot \frac{m_0 \cdot N_p^2 \cdot g \cdot l_t}{b} + 4 \cdot \frac{m_0 \cdot l_t \cdot N_p^2 \cdot m \cdot a}{3b} \qquad (4.3.4.1)$$

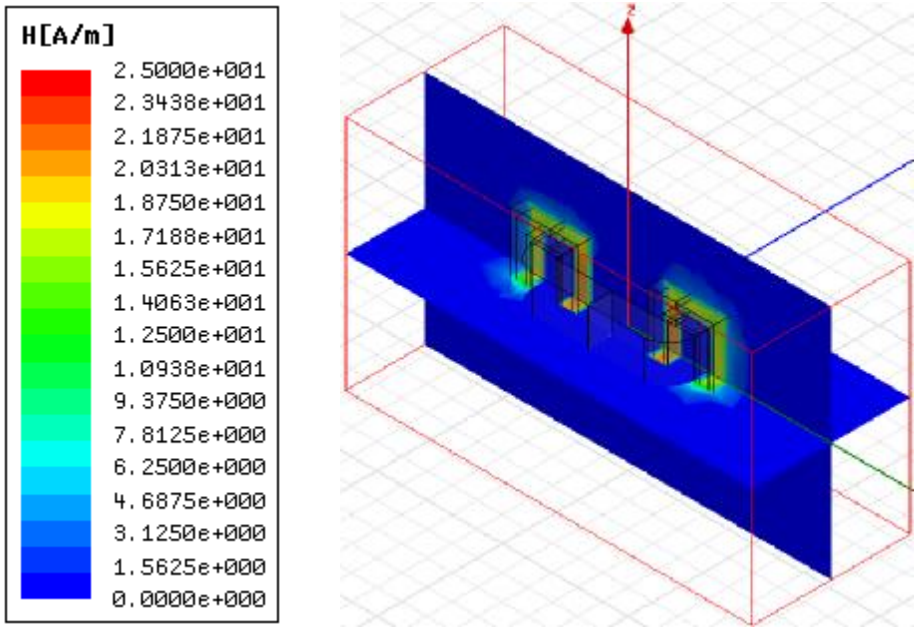

Figure 21 Magnetic field intensity distribution in layered winding with airgap 0.127mm

4.4 Energy Base Magnetizing and leakage inductance Calculation by Simulation

4.4.1 Energy in a Coupled Circuit

We can analyze the magnetic characteristics with software such as Maxwell 3D with finite element method (FEM) based on the stored energies under different excitations. The stored energy in an inductor is given by (5.4.1.1). The stored energy in magnetically coupled coils can be determined by following method.

The magnetically coupled circuit with coils can be represented by Fig.22. The energy stored in the coils is zero with i1 and i2 are zero initially. The power is represented by (5.4.1.2), hence total energy stored in the circuit is (5.4.1.3) if i1 is increased from zero to I1. The mutual voltage induced in coil 2 is $M_{12}\frac{di_2}{dt}$ if i2 is increased from zero to I2 with maintaining i1=I1, while the mutual voltage induced in coil 2 is zero because the i1 does not change. Therefore the power in the coils is (5.4.1.4) and the energy stored in the circuit is (5.4.1.5). The total energy stored in the circuit when the i1 and i2 is constant I1 and I2 respectively is given in (5.4.1.6). We also know that the stored energy in the magnetically coupled coils is same regardless of how to get to the final conditions. The coupling coefficient is a measure of the magnetic coupling between two coils and calculated by (5.4.1.7)

$$w = \frac{1}{2} LI^2 \tag{5.4.1.1}$$

$$p = vi = i \cdot L \frac{di}{dt} \tag{5.4.1.2}$$

$$w_1 = \int p_1 dt = L_1 \int_0^{I_1} i_1 di_1 = \frac{1}{2} \cdot L_1 I_1 \tag{5.4.1.3}$$

$$p_2 = i_1 M_{12} \frac{di_2}{dt} + i_2 v_2 = I_1 M_{12} \frac{di_2}{dt} + i_2 L_2 \frac{di_2}{dt} \tag{5.4.1.4}$$

$$w_2 = \int p_2 dt = M_{12} I_1 \int_0^{I_2} di_2 + L_2 \int_0^{I_2} i_2 di_2 = M_{12} I_1 I_2 + \frac{1}{2} \cdot L_2 I_2^2 \tag{5.4.1.5}$$

$$w_{total} = w_1 + w_2 = \frac{1}{2} \cdot L_1 I_1^2 + \frac{1}{2} \cdot L_2 I_2^2 + M_{12} I_1 I_2 \tag{5.4.1.6}$$

$$k = \frac{M_{12}}{\sqrt{L_1 L_2}} \tag{5.4.1.7}$$

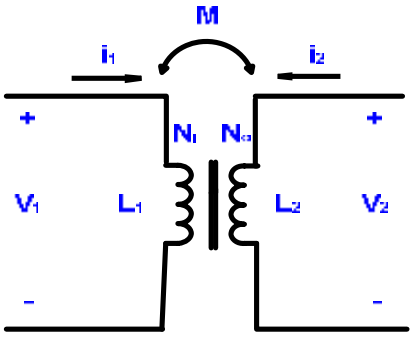

Figure 22 The circuit for deriving energy stored a coupled circuit

4.4.2 Procedure to Calculate the Inductance based on Simulation Data

1. Calculate the self inductances by increasing i_1 from zero to I_1 while $i_2 = 0$.

$$w_1 = \int_0^{I_1} i_1 L_1 \frac{di_1}{dt} dt = \int_0^{I_1} L_i \, i_1 \, di_1 = \frac{1}{2} L_1 I_1^2 \quad \rightarrow \; L_1 \tag{5.4.2.1}$$

$$w_2 = \int_0^{I_2} i_2 \, L_2 \frac{di_2}{dt} dt = \int_0^{I_2} L_2 \, i_2 \, di_2 = \frac{1}{2} L_2 I_2^2 \quad \rightarrow \; L_2 \tag{5.4.2.2}$$

2. Calculate the stored energy by increasing i_2 from zero to I_2 and maintaining $i_1 = I_1$.

$$w_3 = \int_0^{I_2} I_1 M_{12} \frac{di_2}{dt} dt + \int_0^{I_2} i_2 \, L_2 \frac{di_2}{dt} dt = M_{12} I_1 I_2 + \frac{1}{2} L_2 I_2^2 \tag{5.4.2.3}$$

$$w_{total} = M_{12} I_1 I_2 + \frac{1}{2} L_2 I_2^2 + \frac{1}{2} L_1 I_1^2 \rightarrow \; M_{12} \tag{5.4.2.4}$$

The mutual voltage induced in coil 2 is zero since i_1 does not change.

3. Calculate the leakage and magnetizing inductance with coupling coefficient.

$$k = \frac{M_{12}}{\sqrt{L_1 L_2}} \quad \rightarrow \quad L_{Leak1} = (1-k) \times L_1, \;\; L_{Leak2} = (1-k) \times L_2, \;\; L_M = L_1 - L_{Leak1} \tag{5.4.2.5}$$

4.5 Winding capacitance calculation

Stray capacitance was calculated from the simplified model by the assumption above. Each capacitance between adjacent materials is calculated by set up one volt and ground others except the calculation to have capacitances in windings. The voltage difference between turns, winding layers and windings and cores cause these parasitic capacitances. These capacitances can produce large primary current spikes with square wave and electrostatic coupling to other circuit too. Therefore, they cannot be simply ignored in high frequency application, so that predicting and measuring correcting values is very important work especially in high frequency transformer design. The equivalent circuit of transformer is represented by sum of reflected capacitances to appear at the terminals of one winding. It is almost not possible to calculate exact winding capacitance and cannot be simply expressed with simple formula so that capacitances were obtained by MAXWELL 2D electrostatic simulation and compared with the experimental results.

Assumption

1. Each winding are totally symmetrical and equally distributed
2. Cores are considered as ideal conductor.

Air Gap (mm)	Vp=1 , Vcp=-0.5 (Others are	Vs=1 , Vsp=-0.5 (Others are	Vcp=1 (Others are grounded)	Vcs=1 (Others are grounded)	Core_right=1 ,Vsp=1 (Others are
2 Total energy [J]	1.2134e-10	1.1906e-10	5.7560e-10	4.4127e-10	2.9102e-10
1 Total energy [J]	1.2134e-10	1.1906e-10	5.7350e-10	4.4110e-10	5.1506e-10
0.5 Total energy [J]	1.2134e-10	1.1906e-10	5.7069e-10	4.4122e-10	9.5373e-10

Table 12 Energy stored by parasitic capacitances

Air Gap Thickness (mm)	Ca (pF) [error (%)]	Cb (pF) [error (%)]	Cc (pF) [error (%)]	Cd (pF) [error (%)]	Ce (pF) [error (%)]
2	74.8	354.5	98.94	271.7	73.3
1	74.8	353.3	175.1	271.7	73.3
0.5	74.8	351.4	324.4	271.7	73.3

Table 13 Parasitic capacitances of Gen-1 SST transformer

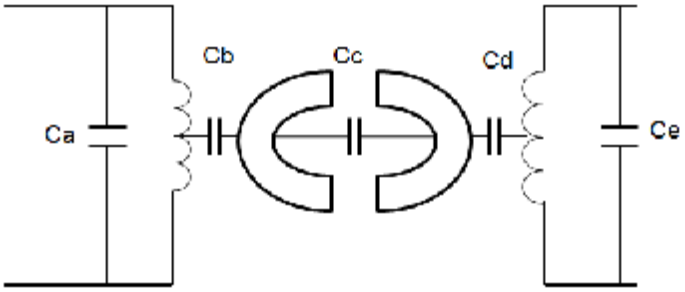

Figure 23 Equivalent circuit for Gen-1 SST transformer

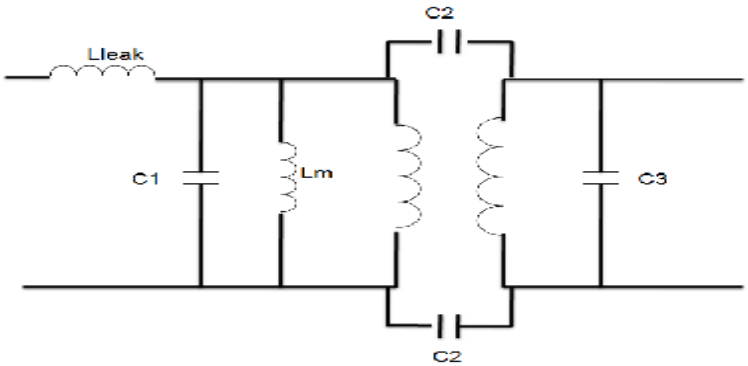

Figure 24 Two winding transformer equivalent circuit

CHAPTER 5

5 LOSS AND ELECTROMAGNETIC ANAYSIS OF COAXIAL WINDING TRANSFORMER DESIGN

The key advantage of coaxial winding transformer is that the inductances and capacitances are predictable with high accuracy because the electromagnetic analysis is relatively simple and can be theoretically calculated simply by hand calculation. Especially, the leakage inductance of transformer is one of the key factors of control strategy in DAB application so that predicting accurate parameters can be a significant advantage for SST high frequency transformer. As we mentioned in core selection section, the coaxial winding transformer has a benefit in size even though it has restraint due to the number of turns. Moreover, the size of external inductors can be reduced because of high operating frequency, so eventually we have a benefit in size as well. We assumed that dc current which might cause the transformer core saturation does not exist in the following calculation. Core loss is one of the most important ac properties of transformers.

5.1 Power Loss

As seen in the previous chapter, nanocrystalline material shows superior performance in terms of power loss. The power loss is relatively less affected by frequency compared to

flux density. Even though low flux density is desirable to reduce core loss, high flux density is required to reduce the number of turns due to the difficulty of physical implementation. When, the core loss per kilogram is 45.05 W/kg and the total mass of 12 toroidal cores of Vitroperm500 is 1.025kg. Therefore, the total core loss is 46.17W.

The copper area of the 0.5mm thickness of cylindrical is approximately $0.493\,cm^2$ Assuming there is no skin and proximity effect, the winding DC loss is

$$Watt/kg = k \cdot f^{(m)} \cdot B_{ac}{}^{(n)} \qquad Vitroperm500: \; k = 0.864e-6,\; m = 1.834,\; n = 2.112 \qquad (5.1.1.)$$

Switching frequency [kHz]	20kHz
Bac [T]	0.83
Mass of a pair of AMCC1000 [kg]	0.0854
Total mass [kg]	1.025
Core loss per kilogram [W/kg]	45.05
Core loss [W]	46.17
Winding loss [W]	15.67
Total loss [W]	61.84

Table 14 Magnetic flux density and core loss

5.2 Inductance Analysis in Coaxial Winding Transformer

5.2.1 Magnetic field distribution in cylindrical structure

The geometry of coaxial transformer can be simplified by ignoring the gap between core and outer winding Fig 25. Magnetic flux density can be represented by simple equation inversely proportional to the core radius in symmetrically cylindrical structure by applying Ampere's law (5.2.1.1).

Assumption

1. The flux density of the core is constant

2. Permeability of core is constant

3. All mutual flux is contained within the transformer core

4. Magnetizing current distribution is cylindrically symmetry.

5. All leakage flux is contained between outer winding and inner winding.

Based on the given assumption above for simplicity, the magnetic flux in each section shown in Fig.30 can be calculated by integration of the flux density in given cross sectional area in terms of the radius. The magnetic flux density in the concentric tubular winding inside window area of toroidal cores is also proved by Maxwell 3D magnetic analysis in Fig.26. The simplified overview of the coaxial winding transformer is shown in Fig.27.

$$B = \frac{m_o m_r N I_m}{2p\,r} \tag{5.2.1.1}$$

$$\Phi_1 = \int_0^{r_{to}} \int_0^{l_{turn}} \left(\frac{p r^2}{p r_{in}^2}\right)^2 \frac{m_0 NI}{2p\,r}\, dh\, dr = \frac{m_0 NI}{8p} l_{turn} \qquad 0 < r < r_{in} \tag{5.2.1.2}$$

$$\Phi_2 = \int_{r_{in}}^{r_{ti}} \int_0^{l_{turn}} \frac{m_0 NI}{2p\,r}\, dr = \frac{m_0 NI}{2p} \ln\left(\frac{r_{ti}}{r_{in}}\right) l_{turn} \qquad r_{in} < r < r_{ti} \tag{5.2.1.3}$$

$$\Phi_3 = \int_{r_{ti}}^{r_{to}} \int_0^{l_{turn}} \left(\frac{p\,(r_{to}^2 - r^2)}{p\,(r_{to}^2 - r_{ti}^2)} \right)^2 \frac{m_0 NI}{2p\,r}\,dr = \frac{m_0 NI}{2p\,(r_{to}^2 - r_{ti}^2)} \left(r_{to}^4 \ln(\frac{r_{to}}{r_{ti}}) - r_{to}^2 (r_{to}^2 - r_{ti}^2) + \frac{1}{4}(r_{to}^4 - r_{ti}^4) \right) l_{turn}$$

$$r_{ti} < r < r_{to} \qquad (5.2.1.4)$$

$$\Phi_4 = \int_{r_{ci}}^{r_{co}} \int_0^{l_{core}} \frac{m_o m_r NI_m}{2p\,r}\,dh\,dr = \frac{l_{core} m_o m_r NI_m}{2p\,r} \ln(\frac{r_{co}}{r_{ci}}) \quad r_{ci} < r < r_{co} \qquad (5.2.1.5)$$

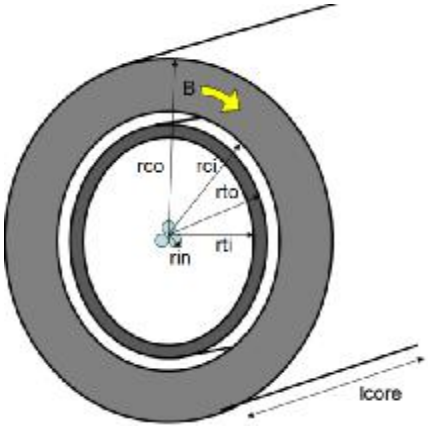

Figure 25 Geometry of coaxial transformer and flux density distribution

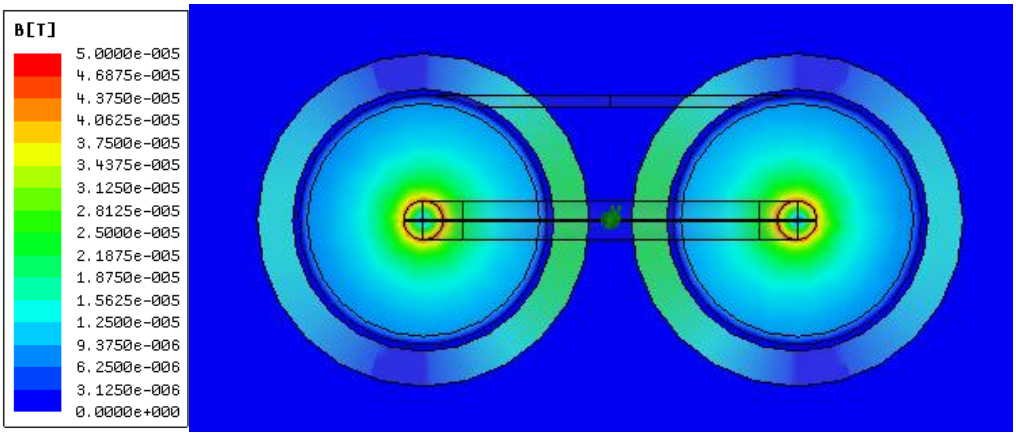

Figure 26 Magnetic flux density distribution of coaxial transformer in profile

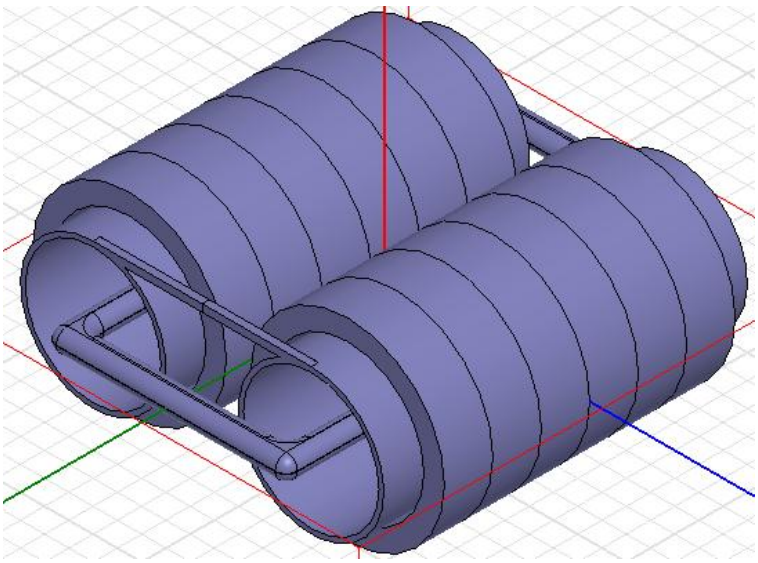

Figure 27 Co-axial Transformer

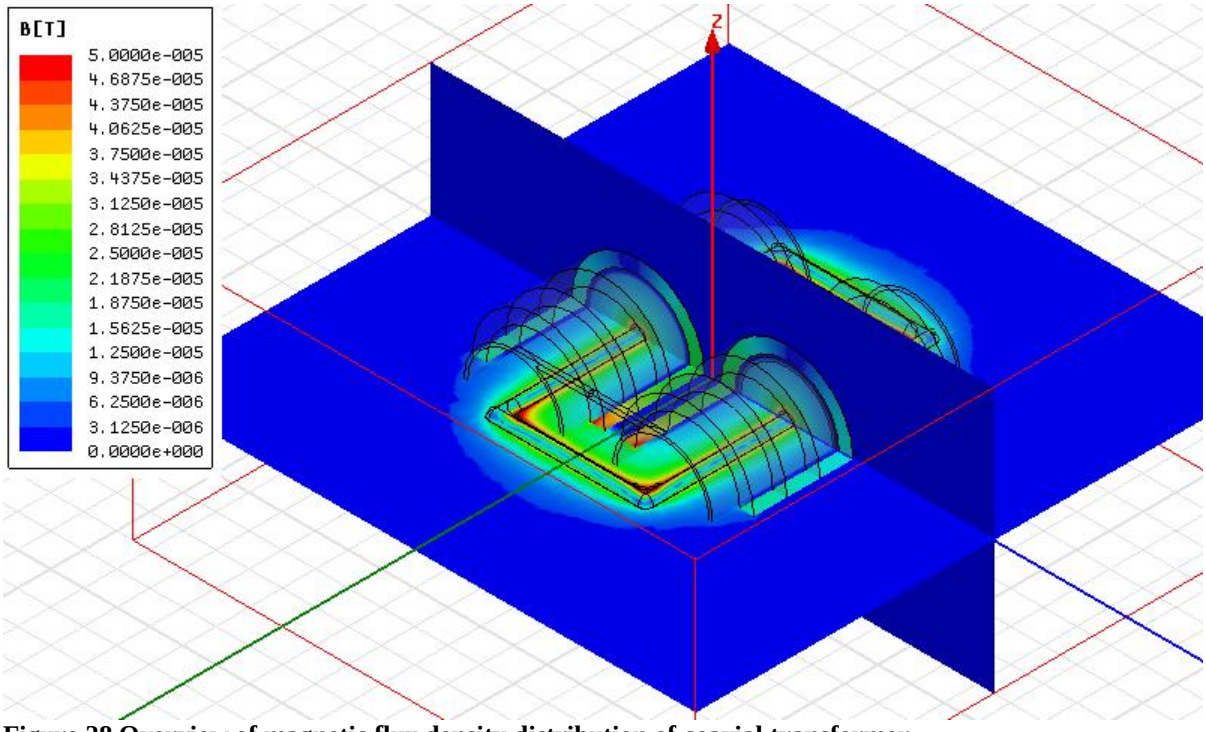

Figure 28 Overview of magnetic flux density distribution of coaxial transformer

5.2.2 **Magnetizing Inductance Analysis**

Assuming all mutual flux is constrained within the transformer cores for simplicity, the total flux linkage is represented by the number of turns times the mutual flux (5.2.2.1). As shown in chapter 5.2.1, the flux in the cores are derived by integrating the flux density on the cross sectional area (5.2.2.2). Inductance is a property to induce electromotive force by the rate of change of the current (5.2.2.4), hence, the magnetizing inductance of coaxial winding transformer is derived (5.2.2.5).

$$\Lambda = N \cdot \Phi \tag{5.2.2.1}$$

$$\Phi = \int_{r_{ci}}^{r_{co}} \int_{0}^{l_{core}} \frac{m_o m_r N I_m}{2p\, r}\, dh\, dr = \frac{l_{core} m_o m_r N I_m}{2p\, r} \ln(\frac{r_{co}}{r_{ci}}) \tag{5.2.2.2}$$

$$v(t) = N \cdot v_{turn}(t) = N \cdot \frac{d\Phi(t)}{dt} = \frac{d\Lambda(t)}{dt} \tag{5.2.2.3}$$

$$N \cdot \frac{d}{dt}\left(\frac{l_{core} m_o m_r N \cdot i(t)}{2p\, r} \ln(\frac{r_{co}}{r_{ci}}) \right) = \frac{l_{core} m_o m_r N^2}{2p\, r} \ln(\frac{r_{co}}{r_{ci}}) \frac{di(t)}{dt} \tag{5.2.2.4}$$

$$L_m = N^2 \frac{l_{core} m_o m_r}{2p} \cdot \ln(\frac{r_{co}}{r_{ci}}) \tag{5.2.2.5}$$

5.3 Leakage Inductance Analysis

The exact leakage inductance can be achieved by analysis by three dimensional point of view because the leakage flux at the ends of the transformer is not be able to be solved in two dimension, nonetheless, the result from the leakage inductance of unit length of the coaxial transformer in two dimension is considerably reliable if the coaxial transformer is long enough. It is reasonable to use the method in two dimensions for SST coaxial transformer because the SST transformer which we designed is fairly long and the ends have a minor effect on the total leakage flux. Therefore, we are going to assume that entire transformer is a perfect coaxial structure without the ends and the entire leakage flux is constrained within the coaxial structure of the length of the actual turns.

The outer windings are thin cylinder made of conductor and the inner windings are wound inside of the cylinder. Magnetic core is located outside of the outer winding cylinder. As assumed in the previous chapters, entire leakage flux of the coaxial transformer is constrained symmetrically in window area of toroidal cores and the leakage flux between outer windings and core is ignored, hence the leakage reactance can be represented on the inner winding side only. The flux in each section is provided at (5.3.1) and the leakage inductance is represented by the number of turns times total flux divided by the current flowing in the inner winding (5.3.2).

$$\Phi_1 = \frac{m_0 NI}{8p} l_{turn},\ \Phi_2 = \frac{m_0 NI}{2p} \ln(\frac{r_{ti}}{r_{in}}) l_{turn},\ \Phi_3 = \left(r_{to}^4 \ln(\frac{r_{to}}{r_{ti}}) - r_{to}^2 (r_{to}^2 - r_{ti}^2) + \frac{1}{4}(r_{to}^4 - r_{ti}^4) \right) l_{turn} \quad (5.3.1)$$

$$L_{leak} = \frac{N(\Phi_1 + \Phi_2 + \Phi_3)}{I} \quad (5.3.2)$$

The leakage reactance is predictable with minor errors thanks to the simple cylindrical geometry. It is very attractive advantage for DAB converter application which uses the leakage inductance as one of the terms to determine the amount of power to transfer from the control point of view rather than just minimizing it.

	Self inductance on HV side [mH]	**Self inductance on LV side [mH]**	**Mutual inductance [mH]** (referred to high voltage side)	**Magnetizing inductance [mH]** (referred to high voltage side)	**Leakage inductance [uH]** (referred to high voltage side)	**Coupling coefficient**
Calculation	331.481	3.6688	0.2293	331.11	328.07	0.9999
simulation	317.738	3.5139	0.2197	317.2035	534.50	0.9994

Table 15 Inductance

CHAPTER 6

6 HIGH VOLTAGE INSULATION

The diverse conditions under high voltage require careful design based on electric field analysis. The insulation materials used for high voltage condition can be gases, vacuum, solid, and liquid or a combination of these. The successful operation of high-voltage power system can be achieved by the correct choice of insulating material and maintaining them in good condition. The major references of insulating materials are permittivity, resistivity, dielectric dissipation factor and partial discharge characteristics. The moisture in the air also plays an important role. The insulation level has to be adjusted by humidity values when testing in high-voltage condition. Oil which is typically used as an insulant can reduce partial discharge and breakdown stresses. The structures of power system equipment must withstand the expected thermal, mechanical and electric stresses between conductors at different potentials. Polypropylene film has high electric strength and low losses so it is used a lot as dielectric in power electronics.

1. Insulation material should be homogeneous. The electric field keeps the same so that the electric field strength gradient is as constant as possible.

2. Derate the dielectric strength of insulation depending on the shape of the conductors.

6.1 Electric Breakdown and Partial Discharge

There are two major concerns in terms of 'high voltage', the possibility of causing a spark in the air and the danger of electric shock by contact or proximity. It needs to be taken care of between two conductors or conductor and ground under high voltage. Even though there is no exact criteria, generally high voltage circuit is defined as those with more than 1000V AC and 1500V DC.

Electrical breakdown is a rapid reduction in the resistance of the insulator that can cause a spark jumping around or though the insulator and partial discharge is localized electrical dielectric breakdown of a small portion of a solid or liquid insulation system between conductors. Air is normally a good insulator but it can begin to break down under stress by a high voltage in electric field strength of more than $3 \cdot 10^6 \ V/m$. The breakdown of the air leads spark or ark that bridges the gap between conductors. The partial discharge occurs when the local electric field intensity exceeds the dielectric strength of the fluid surrounding conductor. The pulse discharge occurs in short time, less than 1us. The intensity is represented by the charge level in picocoulombs or nanocoulombs. The insulation breakdown occurs at the breakdown voltage and results in a short circuit.

Corona discharge is an electric discharge caused by the ionization of a fluid surrounding conductor under high strength of electric field but not as high as it can cause electric breakdown or arcing. The fluid become ionized and conductive when the strength of electric field is large enough and it is affected by geometry because a sharp point has much

higher gradient. Corona discharge can cause power loss, audible noise and most importantly insulation damage which can lead equipment failure.

6.2 Electric Stress Distribution in Multiple Dielectric Insulation System

Even thought the geometry of transformer is complicated and not easily simulated by FEM(Finite Element Method) simulation due to the burden of storage and memory, the design and selection of insulation can be estimated by prior knowledge choosing highest electric stress and simplifying the complicated geometry. Electric stress in parallel and concentric configuration is analyzed by calculation and simulation is conducted with MAXWELL 2D electrostatic field analysis to gain an insight into electric field distribution to choose insulation materials and determine the clearance distance. Edge effect is not easily analyzed by calculation so it is taken care of by MAXWELL 3D electric field simulation for the selective highest electric stress areas of the transformer.

The electric field intensity is the force per unit charge when placed E in the electric field(6.2.1). The electric field intensity is dependent on the medium in which the charge is placed so the electric flux density D is also used (6.2.2).

$$F = qE \tag{6.2.1}$$

$$D = e\,E \tag{6.2.2}$$

The work done on a charge when moved in an electric field is defined as the potential. The electric stress is subjected to the numerically voltage gradient (Electric field intensity). The dielectric strength of an insulation material can be defined as the maximum dielectric strength which the material can withstand. The electric breakdown of insulating materials depends on a variety of parameters, such as field configurations, humidity and surface condition etc.

$$V = \frac{W}{q} = -\int_l E \cdot dl \tag{6.2.3}$$

$$E = -\nabla V \qquad (\nabla = a_x \frac{\partial}{\partial x} + a_y \frac{\partial}{\partial y} + a_z \frac{\partial}{\partial z}) \tag{6.2.4}$$

The field distribution is determined by the Poisson's equation. V is the potential at the given point and r is the charge density in the region, but typically the space charges are not present in case of high voltage apparatus so Laplace's equation can apply for insulation tests.

$$\nabla^2 V = -\frac{r}{e_0} \tag{6.2.5}$$

$$\nabla^2 V = 0 \tag{6.2.6}$$

6.2.1 **Parallel electrode**

The electric stress can be inspected by simple parallel electrode structure in the condition where insulation material is between parallel electrodes by neglecting edge effects. The electric field intensity can be calculated by Poisson's equation. This calculation is an indication of how much distance is required to withstand the potential difference.

$$\begin{cases} V_1 = A_1 x + B_1 & x > a \\ V_2 = A_2 x + B_2 & x < a \end{cases} \tag{6.2.1.1}$$

$$V_1(x=d)=0,\quad V_1(x=a)=V_2(x=a)\quad V_2(x=0)=V_0\quad D_{1n}-D_{2n}=r_{a,x=a}=0 \tag{6.2.2.2}$$

$$E_1=\frac{-V_o}{(a-d)-\frac{e_1}{e_2}a}a_x \qquad E_2=\frac{-V_o}{\frac{e_1}{e_2}(a-d)-a}a_x \tag{6.2.2.3}$$

Figure 29 Geometry of parallel electrode

6.2.2 **Concentric electrode**

The procedure to achieve electric field intensity is basically the same as we did with parallel electrode. Since $r_v = 0$ in this case, Laplace's equation is applied. Radius of the wire on the high voltage side (17AWG 35/32, New England Wire co.) is 0.762mm and the PFA insulation is 0.343mm and the dielectric constant of PFA is 2.03. The electric field intensity of the concentric electrode is derived by Laplace's equation and boundary condition (6.2.2.3).

$$\begin{cases} V_1 = A_1 \ln|r| + B_1 & a < x > b \\ V_2 = A_2 \ln|r| + B_2 & b < x < c \end{cases} \tag{6.2.2.1}$$

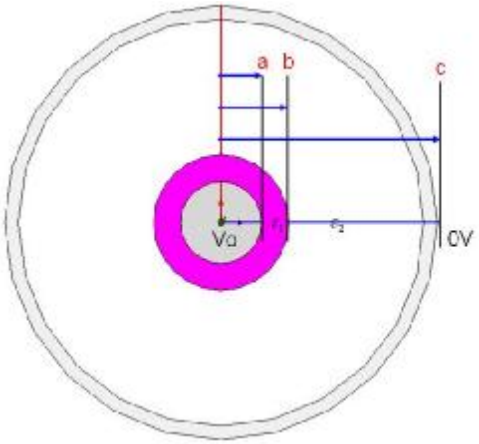

Figure 30 Electrostatic field analysis of wire insulation

$$\begin{cases} E_1 = -A_1 / r & a < r < b \\ E_2 = -A_2 / r & a < r < b \end{cases} \tag{6.2.2.2}$$

$$V_1(r=0) = V_o, \quad V_2(r=c) = 0, \quad V_1(r=b) = V_2(r=b) \tag{6.2.2.3}$$

$$A_1 = \frac{-V}{\ln\frac{b}{a} - \frac{e_1}{e_2}\ln\frac{b}{c}}, \quad A_2 = \frac{-V}{\frac{e_2}{e_1}\ln\frac{b}{a} - \ln\frac{b}{c}} \tag{6.2.2.4}$$

$$E_2(r=b) = \frac{-V}{\frac{e_2}{e_1}\ln\frac{b}{a} - \ln\frac{b}{c}} \cdot \frac{1}{b} \tag{6.2.2.5}$$

6.3 Insulation Strategy

The SST high frequency and high voltage transformer is designed as oil-free type. There are two possible methods considered for Metglas AMCC1000 at frequency of 3 kHz to meet the insulation requirement.

The input of SST is single phase 7.2kV, and the output is 120V/240 with ground line. The AC-DC stage consists of three cascaded full bridges. The topology for DC-DC stage is three dual active bridges with output paralleled to provide a DC-link for output stage, which is a three-leg two-phase inverter. The transformer in each stage provides voltage transfer between 3.8kV in primary side and 400V in secondary side DC-link. The switching frequency for high voltage side semiconductor devices is set to 1-3 kHz due to the frequency capability limit of 6.5kV IGBT's. The high voltage issues are necessarily taken care of because the high frequency transformer for SST application is require to support approximately 15kV with 30% margin in worst case. The specification for the high frequency transformer in solid state transformer is summarized as follows:

Frequency	HV DC link	LV DC link	Power Rating	Turns Ratio	Isolation requirement	Allowed temp. rise
1~3kHz	3800V	400V	20/3=7kVA	3800/400=9.5	15kV	40

Table 16 Insulation requirement

Firstly, the primary core is electrically connected to negative terminal of DC-link in each stage, so the insulation requirement of primary winding to core is reduced. The secondary core is electrically connected to output neutral point or the negative terminal of DC-link of its lower level cascaded stage. Thus, the common mode high voltage referred to ground is evenly distributed though primary winding, primary core, secondary core and secondary winding Fig.37. We can have more room for windings thanks to the less electrical stress between core and windings. Nonetheless, there is a thin insulation layer, such as polypropylene film or plate, in the airgap between two C cores, so high electric field occurs at the corner and edges area of air gap, which might potentially cause corona effect. These parts should be sealed with solid insulation potting material. The transformer made this method will be first candidate called Model-1 for SST high frequency and high voltage transformer.

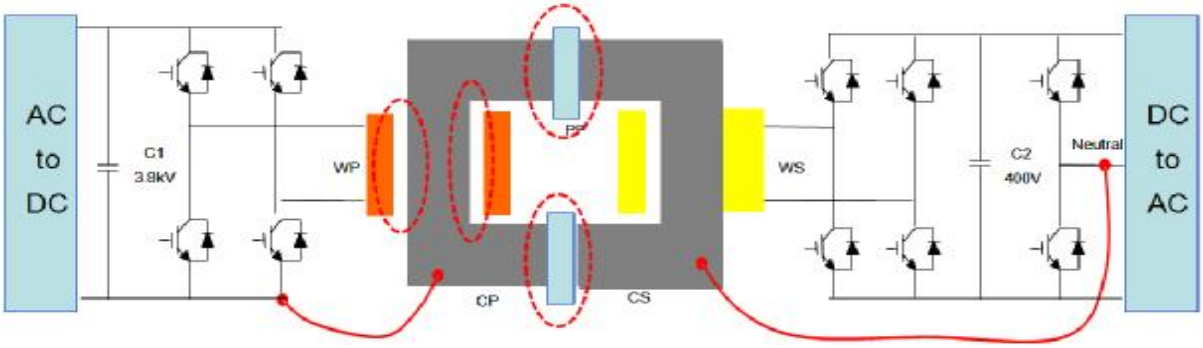

Figure 31 Proposed oil-free insulation strategies for design-1

As shown in Fig 32, the electric field intensity on the surface of insulation is around 2MV/m, so there is around 50% margin at the distance of 4mm between concentric electrodes. The electric field intensity on the surface reaches to the air breakdown point when the distance between the concentric electrodes is 1.7mm at 3.8kDC.

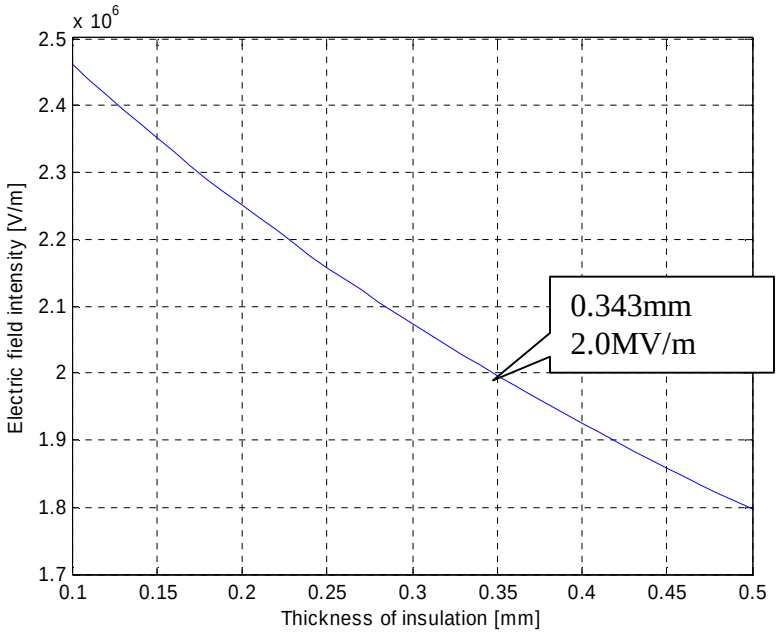

Figure 32 Electric field intensity on the surface in terms of thickness of insulation.
(17AWG 35/32. Concentric electrodes. Distance between ground and insulation: 4mm, Vo=3.8kV)

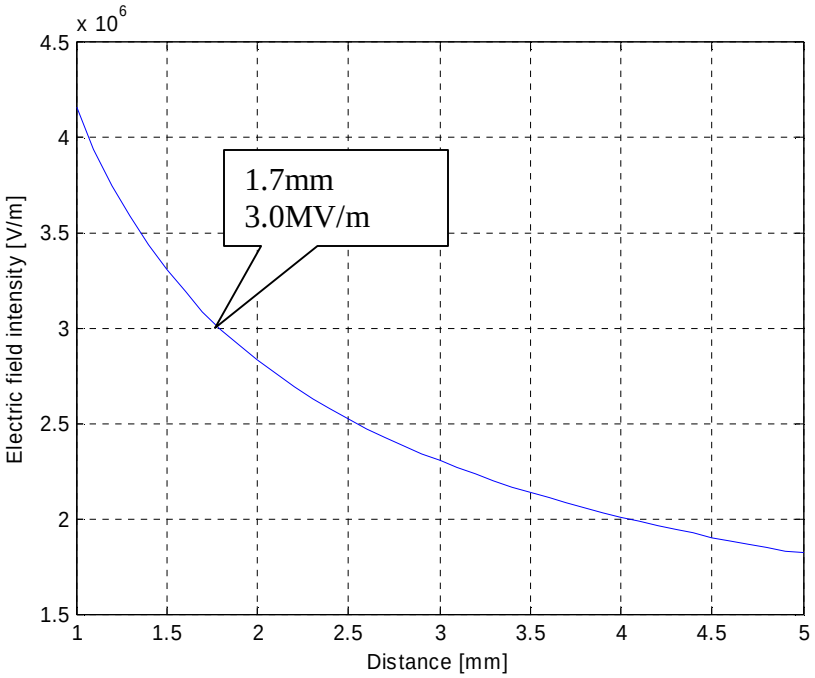

Figure 33 Electric field intensity on the surface in terms of the distance
(17AWG 35/32. Cylindrical shape. Insulation thickness: 0.343mm, Vo=3.8kV)

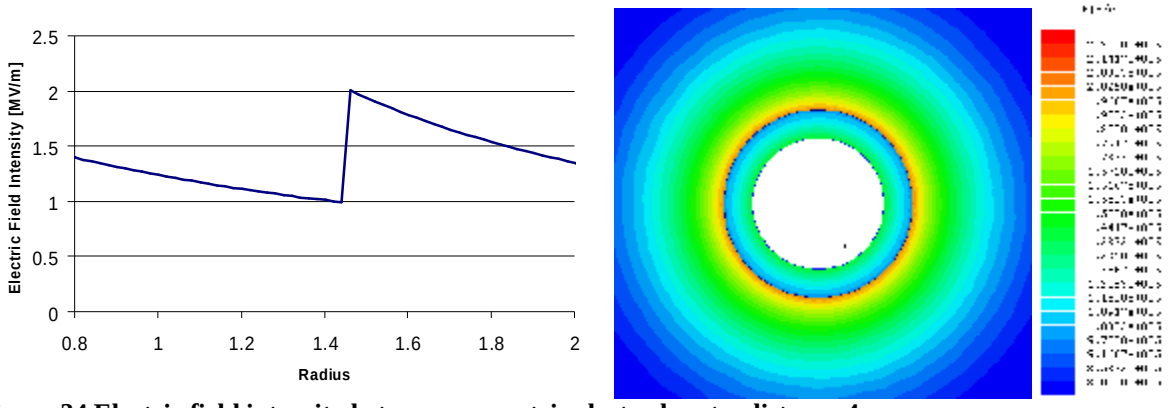

Figure 34 Electric field intensity between concentric electrodes at a distance 4mm
(17AWG 35/32. PFA insulation thickness: 0.343mm Calculation (left), Simulation (right))

There is possibility that the airgap insulation causes more serious problem than the insulation between cores and windings on high voltage side. Hence, we are going to ground

both cores, so there becomes no electrical stress between cores anymore. However, enough room between core and winding on the high voltage side has to be guaranteed to support even higher electric stress. Additionally, the reduction of the number of turns to have more margin makes the flux density higher and core loss increass. This method is used for Model-2 SST transformer.

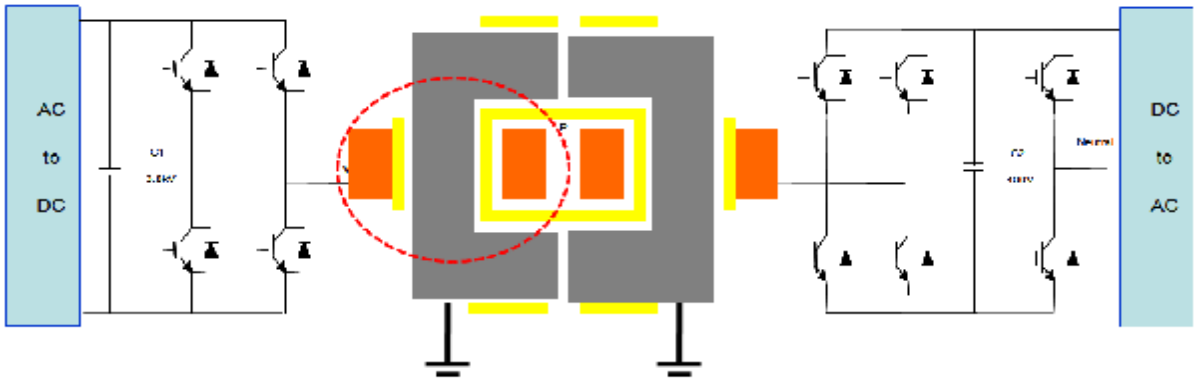

Figure 35 Proposed oil-free insulation strategies for design-2

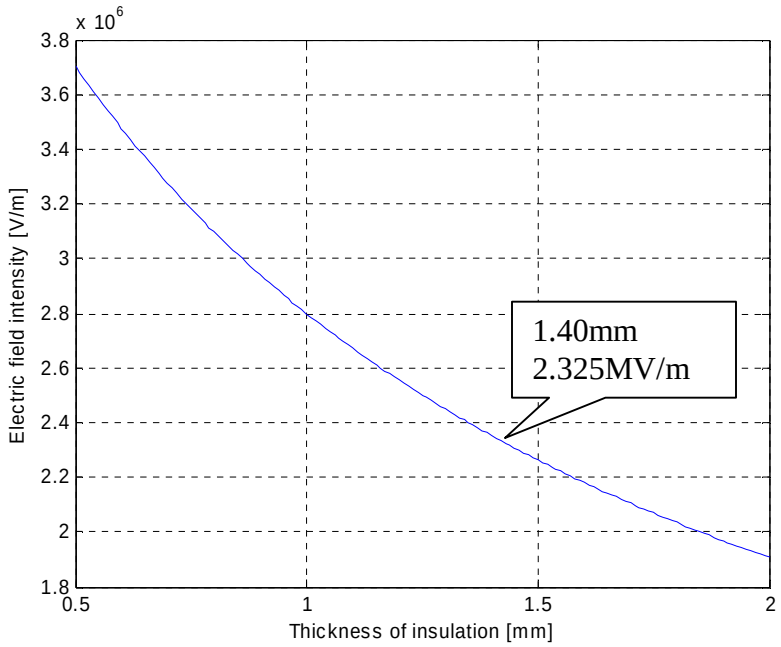

Figure 36 Electric field intensity on the surface in terms of the thickness of insulation.
(17AWG 35/32. Concentric electrodes. Distance between ground and insulation: 10mm, Vo=3*3.8kV)

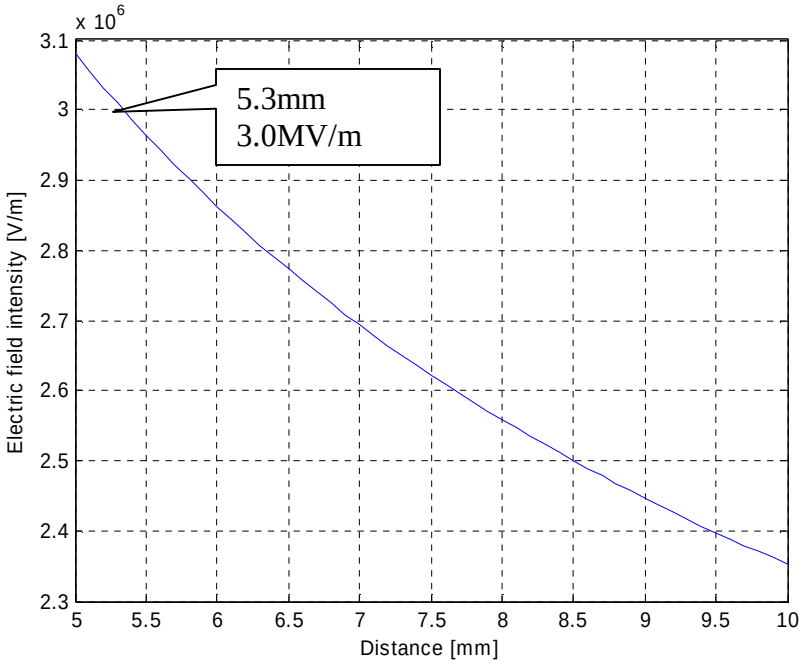

Figure 37 Electric field intensity on the surface in terms of the distance
(17AWG 35/32. Cylindrical shape. insulation thickness: 2.0mm, Vo=3*3.8kV)

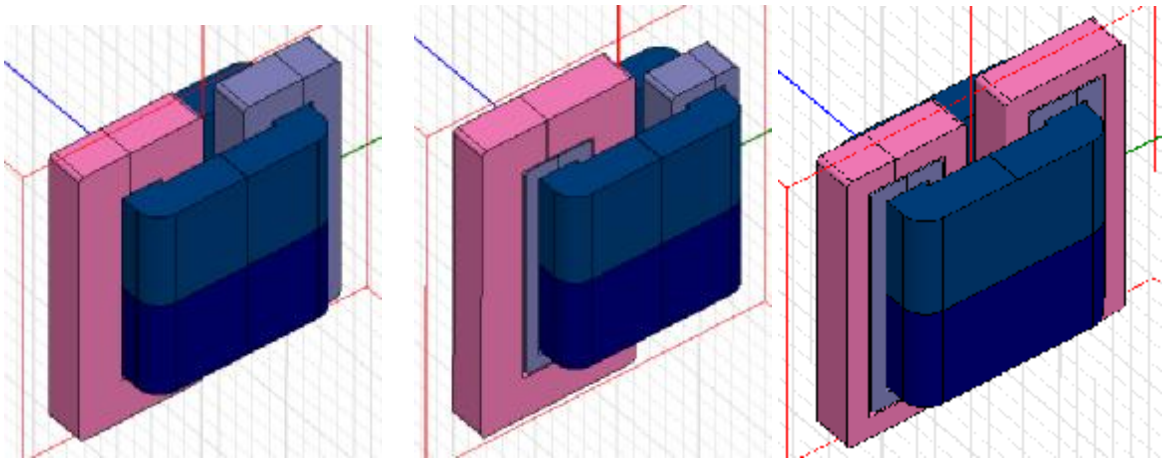

Figure 38 Ex. 1 (top left), Ex. 2 (top right), Ex. 3 (bottom left)

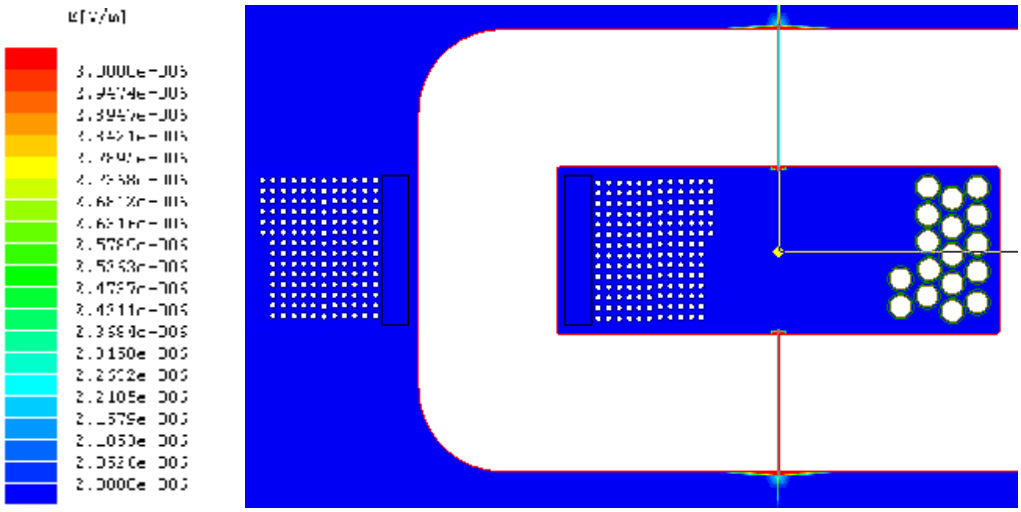

Figure 39 Electric field intensity distribution of Ex 1

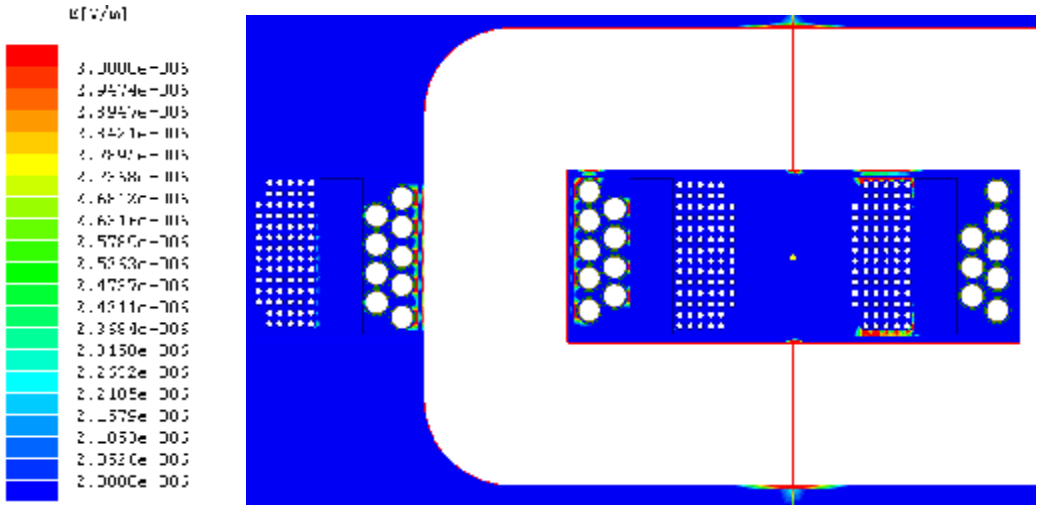

Figure 40 Electric field intensity distribution of Ex 2

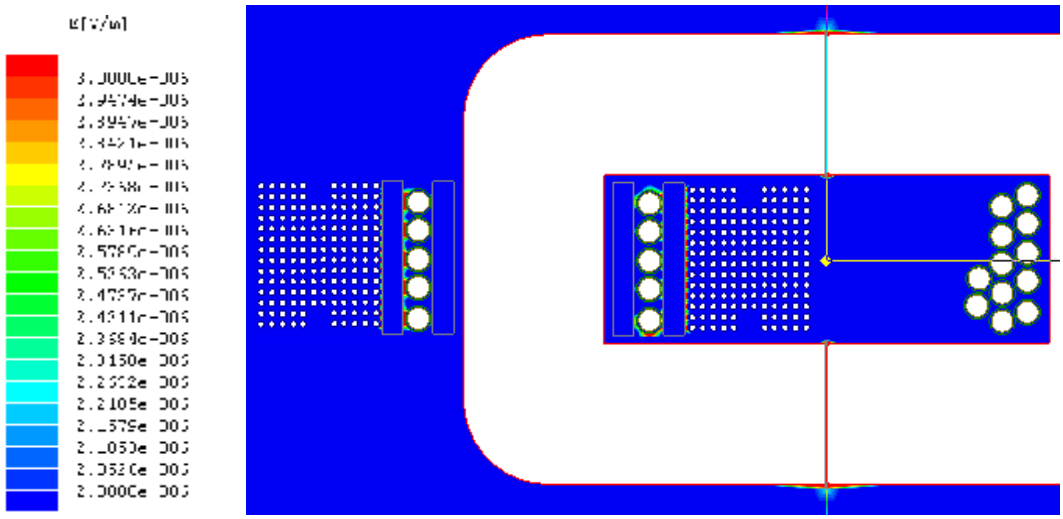

Figure 41 Electric field intensity distribution of Ex 3

CHAPTER 7

7 TRANSFORMER DESIGN PROCEDURE

The main reason why designer prefer high operating frequency is size reduction because the passive components like transformers are typically the bulkiest part of the switching converter circuit. The SST high frequency transformer also pursues compact size than any other factors. High frequency makes the flux linkage small which would reduce the cross sectional area and window area due to the reduction of the number of turns in exchange of core loss. There are major four variables, flux density, frequency, the number of turns and cross sectional area of cores and they are all non-linear and corresponds each other. We will see the relationship between these four variables to optimize all parameters by eliminating each value step by step.

7.1 Area Product and Power Capability

One of the most popular methods to estimate and initialize the size of core and power capability is area product which is stated as (7.1.1). This equation is in terms of power rating, flux density, frequency, current density, waveform coefficient Kf (K_f = 4.00 for square wave, 4.44 for sine wave), fill factor Ku which is the ratio between window area and copper area. This value does not mean exact size of the core, nonetheless, it helps the designer to select a core by window area and cross sectional area provided by catalog. All

parameters are interrelated to each other so it is very difficult to find right models at once. Generally, many trial-and-errors are required to find best fit to meet the requirement.

$$A_p = W_a \cdot A_c = \frac{(P_{in} + P_{out}) \cdot 10^4}{B_{ac} \cdot f \cdot J \cdot K_f \cdot K_u} \tag{7.1.1}$$

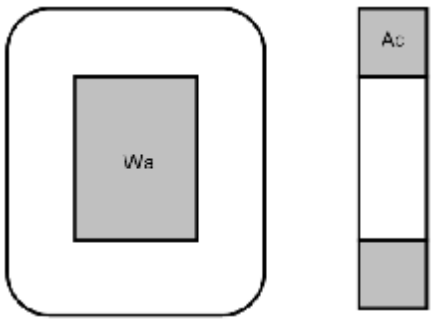

Figure 42 C-core outline showing the window area and cross section

7.2 Relationship between the Flux Density and the Voltage

The integration of voltage during the positive portion of the waveform is flux-linkage, so called volt-seconds (7.2.1). By Faraday's law, the peak value of the ac component of the flux density is obtained by (7.2.2). Transformer designer also need to know to look at the circuit which the transformer will be connected to and work with because the frequency and voltage is determined by the topology or the capability of device in the system. This equation plays an important role and gives an insight to design transformer to meet the required specification. There are exceptional cases that the flux density contains DC components, such as the forward converter which does not allow negative flux density. The DC components do

not affect core loss and performance much but it should be carefully designed for flux density not to reach the saturation point during operation. The SST high frequency transformer is placed between dual active bridges, so the voltage wave form is square wave. Therefore, we can derive the general equation in terms of frequency, the number of turns, cross-sectional area and voltage rating (7.2.3). The magnetizing current is not directly dependent on the winding current but the applied voltage waveform, so the flux density and magnetizing current can reach the saturation point when the applied voltage-second is too large. This is an iterative process to have optimized Bac and the number of turns and size.

$$volt-\sec ond \quad l = \int_{t1}^{t2} v(t)\,dt \tag{7.2.1}$$

$$\Delta B = \frac{l}{2N \cdot A_c} \rightarrow \frac{V}{4f \cdot N \cdot A_c} \text{ (square wave)} \tag{7.2.2}$$

$$V = 4B_{ac} \cdot f \cdot N \cdot A_c \tag{7.2.3}$$

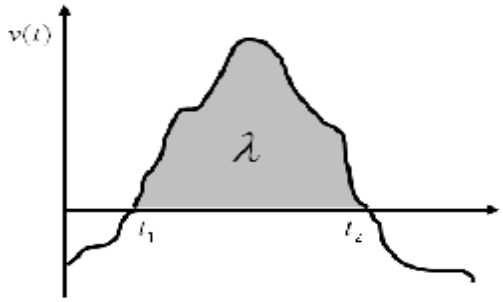

Figure 43 Transformer voltage waveforms, illustrating the volt-seconds

7.3 Relationship between Frequency, Flux density and the Number of Turns

The key parameters to design transformer are frequency, flux density and the number of turns. These three parameters corresponds to each other, so there is no way to determine these values at once. For now, the operating frequency and voltage rating are already chosen, hence the degree of freedom is still two, and we can step forward by selecting each parameter step by step. In case of the flux density, there is another important concern not to make the transformer saturate. When the flux density exceeds the saturation flux density of the material, the magnetizing inductance becomes small and the magnetizing current becomes large, which can short the transformer winding. Increasing frequency can lead small size but increase the loss significantly so core material which has very low core loss, such as nonocrystalline, is necessarily required. Additionally, magnetic phenomenon like skin effect or proximity effect has to be taken care of. The frequency is also limited by the capability of the switching devices as well. Generally, many trial-and-errors are required to meet the requirement and optimize the values to reduce size, loss and cost as well. Based on the optimization which will be shown in section 2.3, the number of turns on the high voltage side and low voltage side are 190 and 20 respectively with optimized flux density of 0.23 Tesla. Fig. 44 gives the basic concept of the relationship between the parameters to have an insight to design transformers. Assuming the voltage provided to transformer is fixed by an independent source, the three key parameters are all inversely proportional and interact. The

frequency and flux density directly affect the core loss and size, which are inversely proportional each other. Core losses are relatively higher than winding losses in low current operating conditions, therefore, the highest concern has to be taken to core loss and size for the SST high frequency transformer.

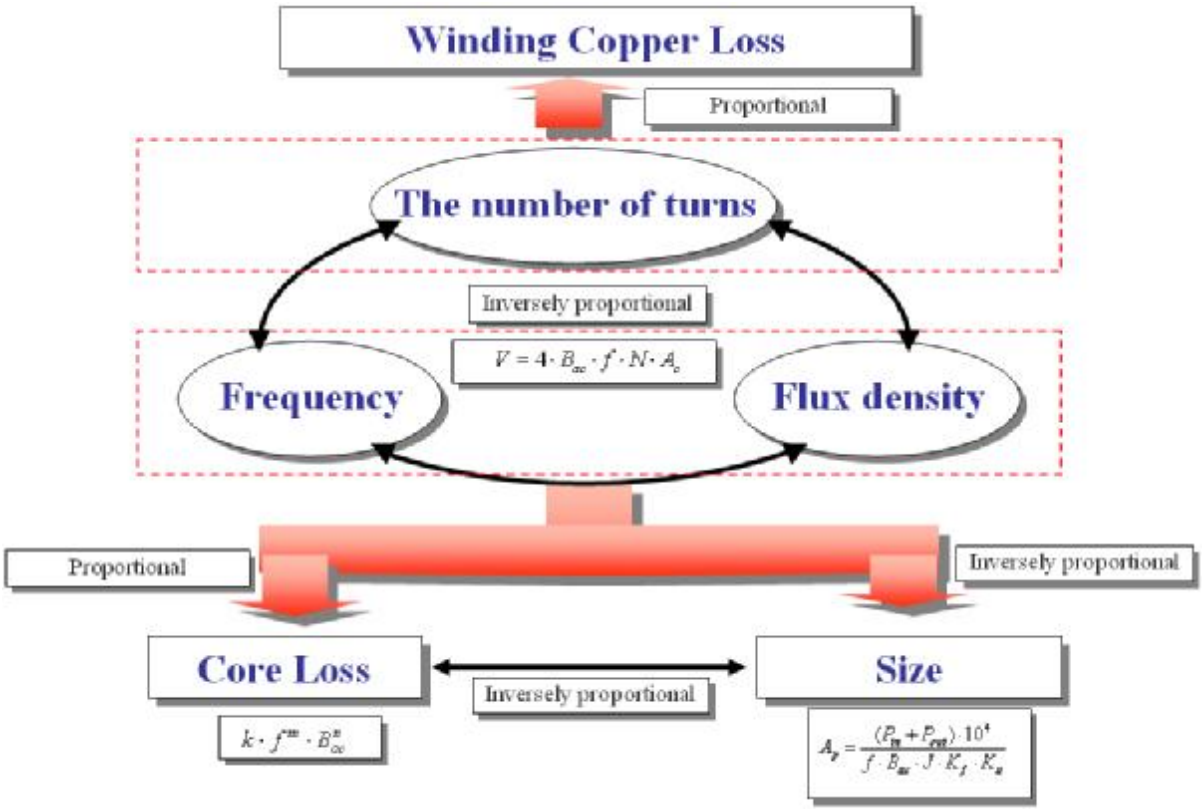

Figure 44 Diagram illustrating the relationship between frequency, flux density and the number of turns

7.4 Core loss and Size with respect to Frequency, Flux density

There are many factors to be considered for transformer designer to select core material and specification. Most importantly, the core losses at high operating frequencies, saturation density which has to made sure not to exceed saturation density and also the influence on core losses are required, additionally, it will be better if the transformer has good thermal and mechanical properties as well. The core material was already decided in chapter 3, we are going to decide the specification of geometry in detail and choose models commercially available

7.5 Solenoidal Winding Transformer Model-1 and Model-2 Design Result

7.5.1 Comparison with respect to the number of cores

The designer has to put the different priority to each variable to finalize all variables with higher optimization. Size is one of the main concerns to design the SST transformer, therefore we decided to put higher priority to the size, precisely cross sectional area of the core, and fix the value first. Additionally, the thickness of airgap is necessarily required to be wider than 0.5mm because of the polypropylene material which is going to be used for airgap, can support around 11kV with 0.5mm. This airgap can significantly reduce magnetizing

inductance. The required leakage inductance at frequency 3 kHz is more than 40mH, so magnetizing inductance need to be approximately more than 400mH considering maximum 10 % of leakage inductance included. As discussed in the previous chapters, 2 or 3 pairs of cores are required to be capable of the power rating of Gen-1 SST. The magnetizing inductance of transformer consisted of 2 pairs is around 210mH, which is two third of 3 pair of core due to the cross sectional area reduction, based on simulation data. Only one way to increase magnetizing inductance is to increase the number of turns but then the number of turn is over 200, which will not physically fit in window area of AMCC1000. By adding one more pairs of C-core, it leads the Bac operating point close to optimization point and, additionally, the leakage inductance of transformer becomes around 50mH, and then the external inductor can be possibly eliminated. Consequently, size can be almost the same or less than transformer with 2-pair core. The core loss of 3-pair cores is going to be almost a half with flux density reduction and also additional advantage of avoiding the temperature rise due to the lower volume and high energy loss which transfer to heat. The specifications are shown in Table 17 and 18. 3 pairs of cores are going to be used for the SST high frequency transformer.

Transformer		
	2 pair	**3 pair**
Core material	**Amorphous Alloy AMCC1000**	**Amorphous Alloy AMCC1000**
Bac [T]	0.41	0.23
Core type	C-Core	C-Core
Cross section area	48.1 cm^2	72.15 cm^2
Window area	42 cm^2	42 cm^2
Ap [cm^4]	2020	3030
Core volume [cm^3]	3015	4522
Core mass [Kg]	14.22	21.33
Number of primary turns	190	190
Number of secondary turns	20	20
primary winding	19/29	19/29
secondary winding	60/27	60/27
primary OD [cm]	0.271	0.271
secondary OD [cm]	0.489	0.489

Table 17 Comparison between 2 pairs and 3 pairs application

	2 pair	**3 pair**
Core loss [W]	102.90	56.45
Winding loss [W]	23.31	32.66
Total loss [W]	126.2	89.11
Self inductance	233.98mH	354.09mH
Coupling coefficient	0.9207	0.9306
Magnetizing inductance	215.42mH (airgap 0.5mm each side)	329.52mH (airgap 0.5mm each side)
Leakage inductance	37.12mH (airgap 0.5mm each side)	49.15mH (airgap 0.5mm each side)

Table 18 Loss comparison between 2 pairs and 3 pairs application

7.5.2 **The number of turns vs. Leakage inductance and core loss**

The geometry of cores, voltage rating and the operating frequency is now fixed, then the degree of freedom becomes only one because the last variable is determined once we choose one of the two variables, the flux density and the number of turns. The final design is determined by these two variables, so we have to make sure all possible conditions, such as core saturation, power loss, high voltage insulation and mechanical fitness as well, at this point.

The leakage inductance and the core loss can be calculated in terms of the number of turns of Design-1 separate winding transformer in Fig.45. It is possible to choose leakage inductance in the range of 40~70mH which DAB converter require to operate properly by selecting the number of turns. The physical limitation of the number of turns is around 200, therefore we can eliminate the external leakage inductance in the range of 170~200 turns with reasonable power loss around 50W/kg.

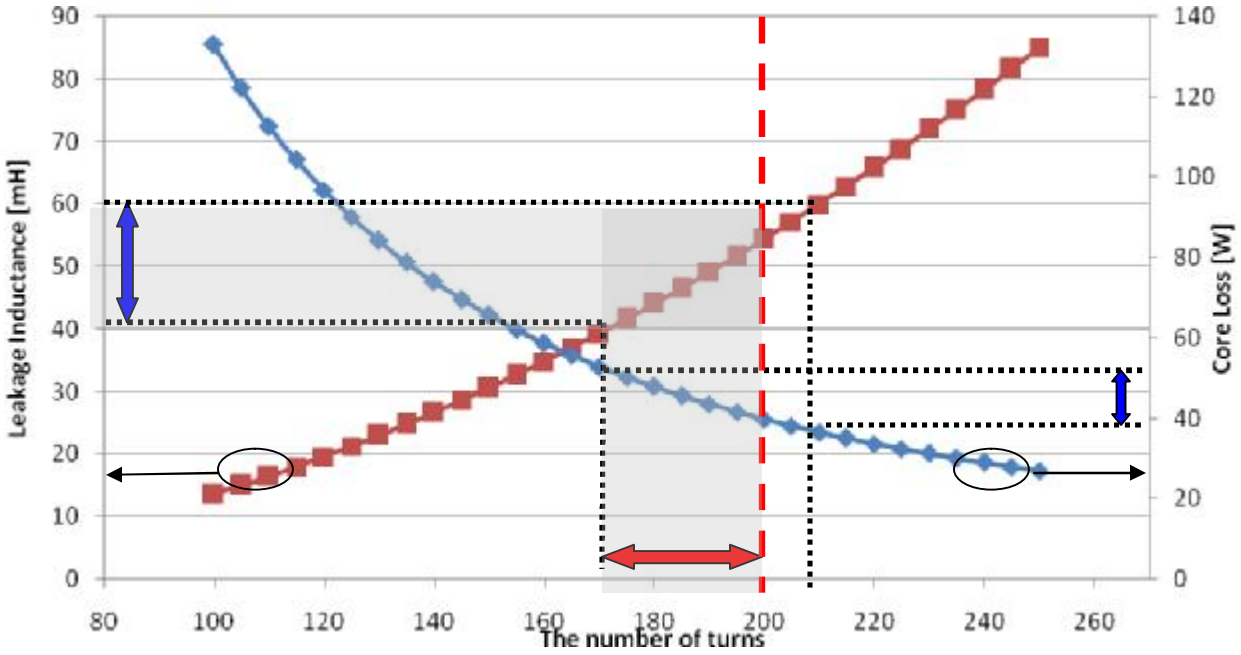

Figure 45 The number of turns vs. Leakage inductance and Core loss of the Design -1

In case of Design-2, more distance is required between cores and windings because of the higher electric potential difference. The leakage inductance of Design-2 is already very low, so it is not considered here and external inductor is necessarily added. The targeting number of turns is between 90 and 110.

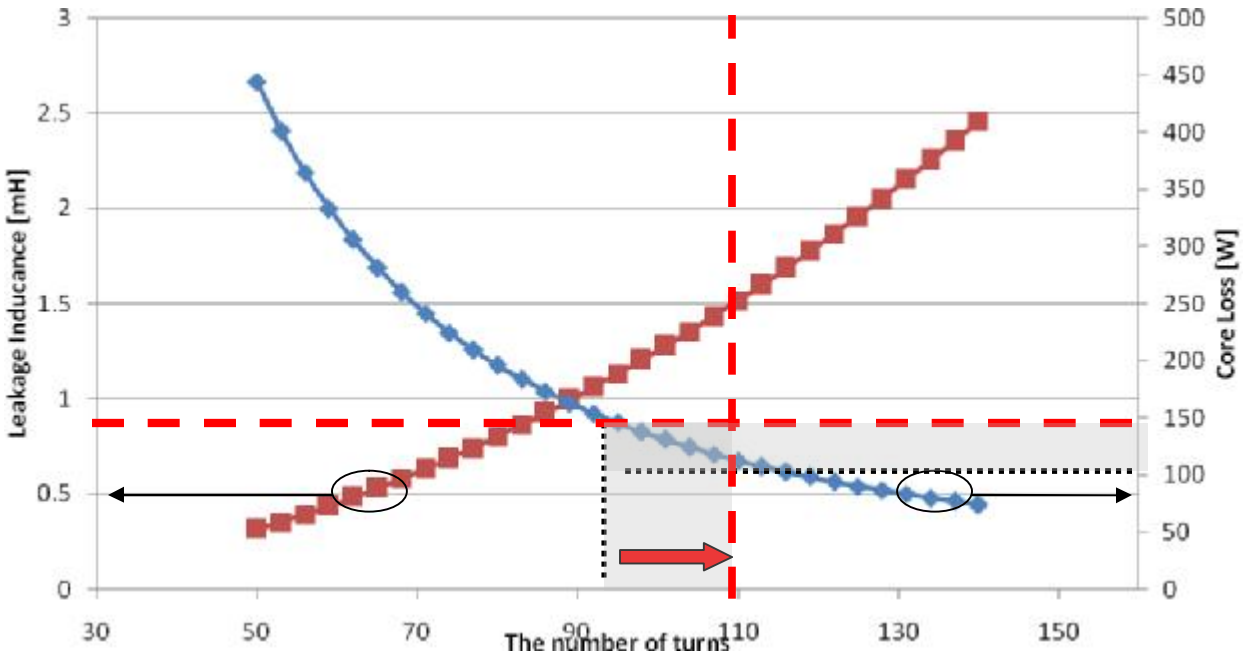

Figure 46 The number of turns vs. Leakage inductance and Core loss of the Design -2

7.5.3 **The number of turns vs. Magnetizing inductance**

Finally, magnetizing inductance is going to be checked in terms of number of turns and thickness of airgap. As discussed in previous chapter, the number of turns has to be between 170~200 and the airgap thickness has to be more than 0.5mm because the airgap made of polypropylene has to be more than 0.5mm to support 11.4kV. The magnetizing inductance also determined by the thickness of airgap and around 300mH is required to keep approximately 10% increase of switching loss in the DAB. The sky blue contour line indicates approximately magnetizing inductance of 300mH. Design-1 has to be placed around the red spot in Fig.47.

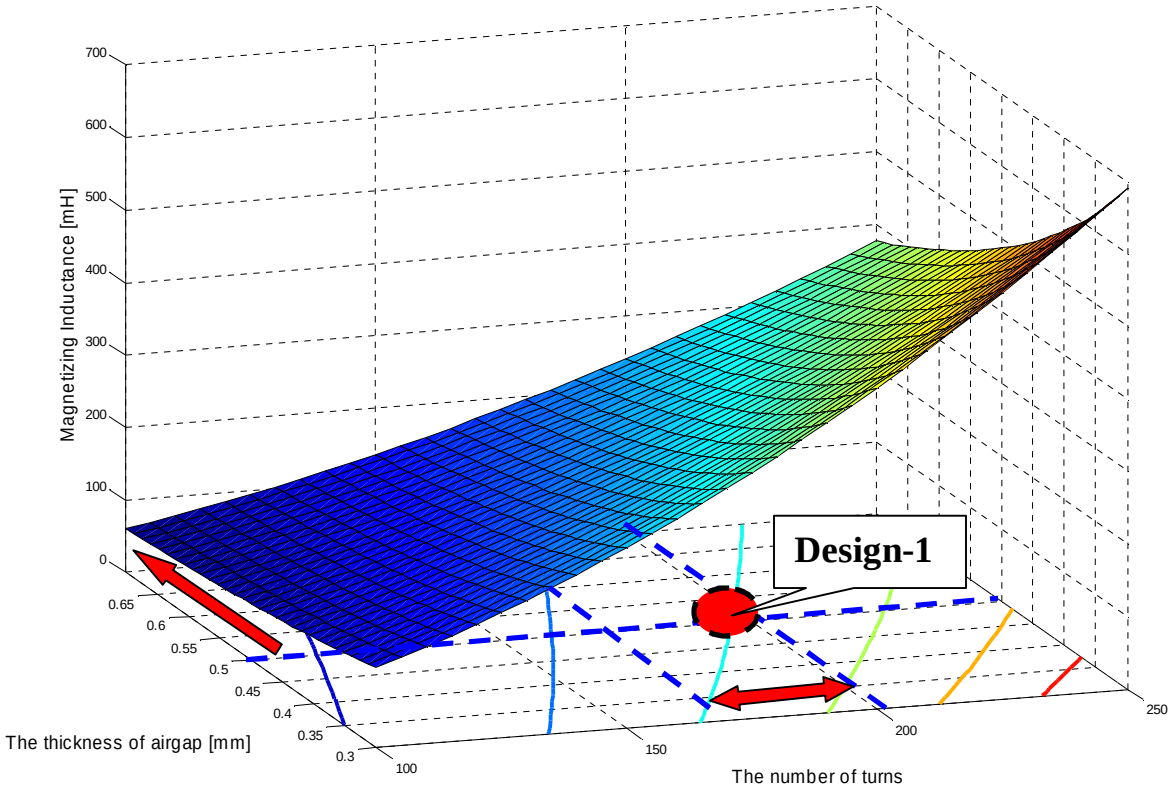

Figure 47 The number of turns and the thickness of airgap vs. Magnetizing inductance of the separate winding transformer

Fig. 48 shows the operating condition of Design-2. Considering the sky blue contour line as criterion of magnetizing inductance, we can select around 110 turns with small airgap because there is no electric stress at airgap of Model-2 application.

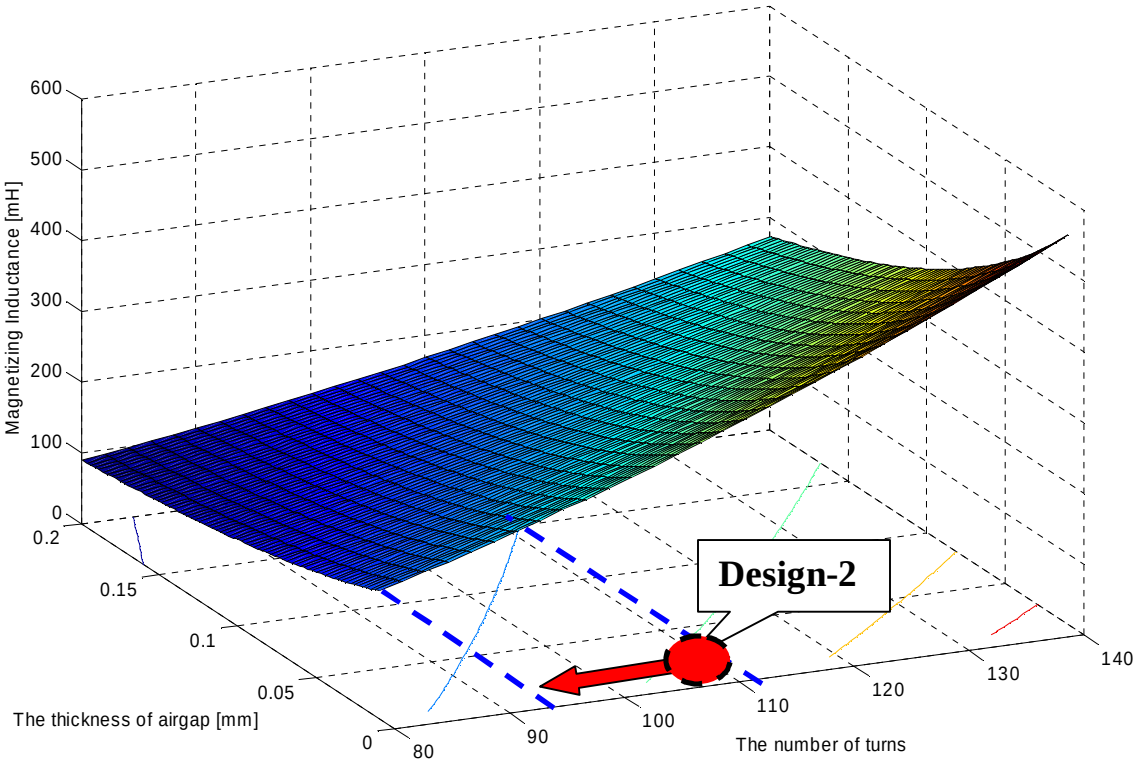

Figure 48 The number of turns and the thickness of airgap vs. Magnetizing inductance of the layered winding transformer

7.5.4 **Bac Optimization**

Saturation flux density and core loss is one of the key trade-offs to design transformers. High saturation flux density can reduce the size, weight and the number of turns but it also leads high eddy current loss in cores. Amorphous alloy 2605SA1 has a relatively high saturation flux density (1.56T) but it needs to be optimized to reduce total

losses of transformer. Total loss is generally presented by the sum of core loss and the winding loss (7.5.4.1). The optimum Bac does not necessarily occurs when the core and winding loss is the same, but when the derivative of the total loss is zero (7.5.4.2). The core loss equation is achieved from datasheet and the winding loss equation was simplified for convenience by ignoring skin and proximity effect because the skin and proximity effect is not significant at the operating frequency of 3kHz as will be shown in winding loss section (7.5.4.4). Suppose that AMCC1000 C-cores are used as decided, the value of Bac needs to be reduced by increasing switching frequency to have a minimum total loss. At frequency of 3kHz, total loss is minimized at Bac of approximately 0.14 according to Bac optimized curve, but window area cannot be capable of the number of turns due to high voltage and low current rating, as long as commercially available AMCC cores are used. Hence, Bac of 0.23 T is chosen instead for this application because the core loss does not make much difference and the number of turns is adjusted to fit in the window area of AMCC1000. Even though there is around 10W additional loss but size remains small.

$$P_{total} = P_{core} + P_{winding} \tag{7.5.4.1}$$

$$\frac{dP_{total}}{dB_{ac}} = \frac{dP_{core}}{dB_{ac}} + \frac{dP_{winding}}{dB_{ac}} = 0 \tag{7.5.4.2}$$

$$p_{core}[W] = k \times f^{m}[kHz] \times B_{ac}^{n}[T] \times mass[kg] \quad \text{(k=6.5, m=1.51, n=1.74)} \tag{7.5.4.3}$$

$$p_{winding}[W] = \frac{V_{in} \cdot 10^{4}}{4 \cdot A_c \cdot B_{ac} \cdot f} \cdot r \cdot MLT \cdot I_{rms}^{2} \tag{7.5.4.4}$$

$$B_{ac}^{n+1} = \frac{V_{in} \cdot 10^4 \cdot 1000^m \cdot MLTp \cdot r_p \cdot I_p^2 + V_{out} \cdot 10^4 \cdot 1000^m \cdot MLTs \cdot r_s \cdot I_s^2}{4 \cdot A_c \cdot f^{m+1} \cdot k \cdot n \cdot total\ mass} \qquad (7.5.4.5)$$

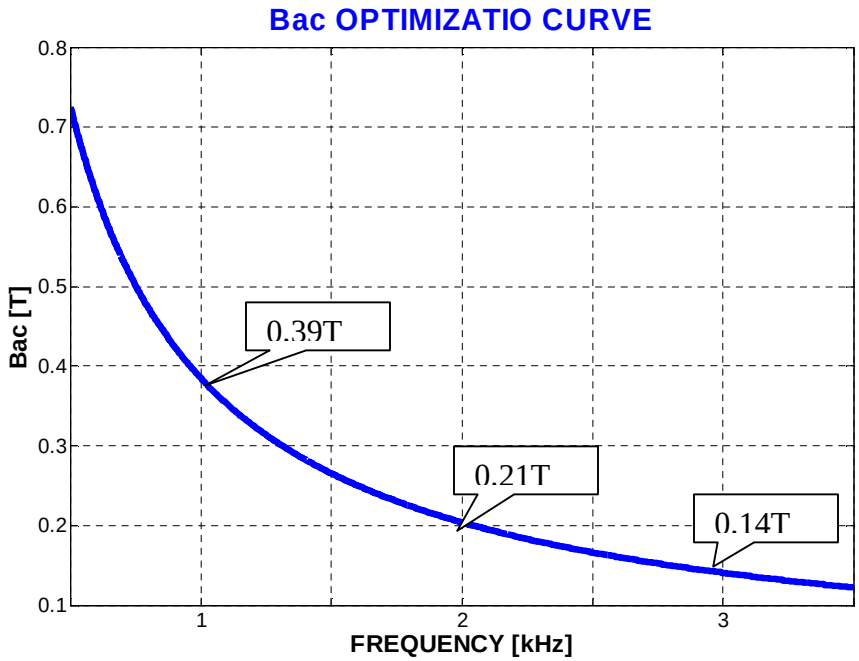

Figure 49 Bac Optimization Curve

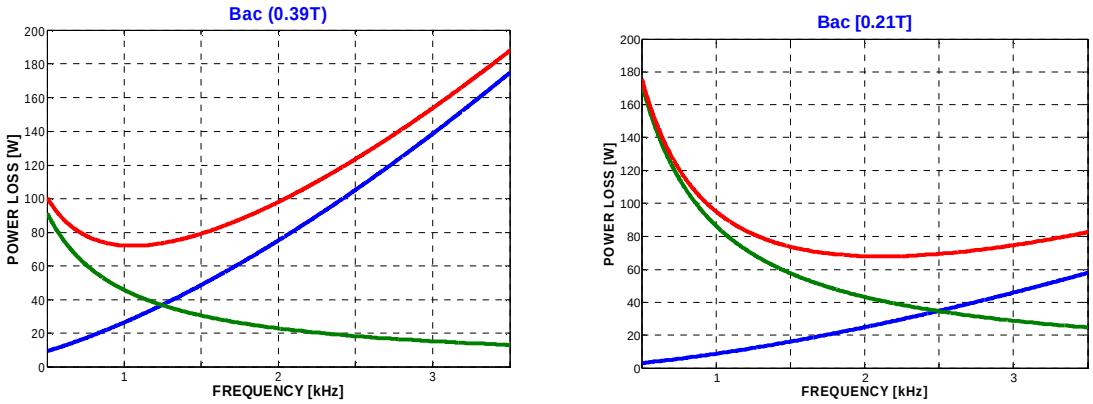

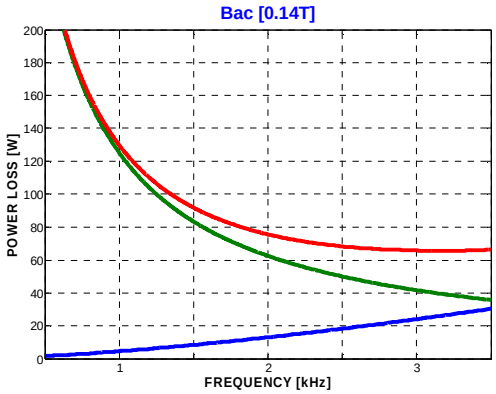

Figure 50 Total loss(red), core loss(blue), winding loss(green) – Bac 0.39(top left), Bac 0.21(top right), Bac0.14 (bottom)

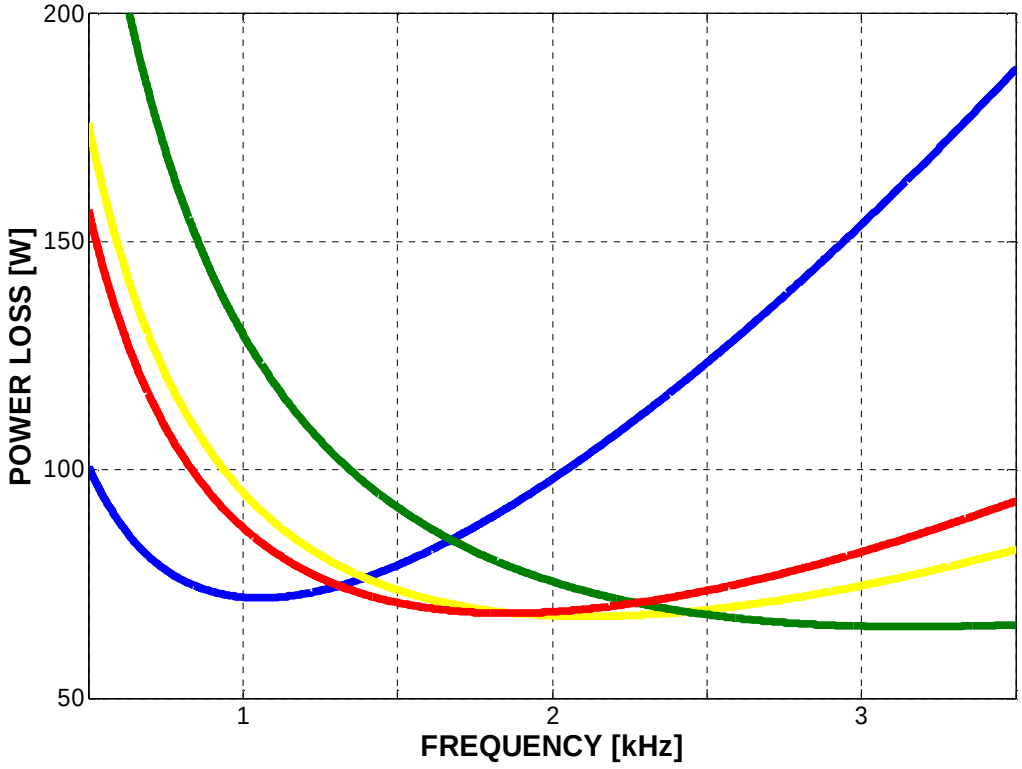

Figure 51 Total power loss at the optimal Bac – Bac 0.39 (blue), Bac 0.21 (yellow), Bac 0.14 (green), Bac0.23(red)

7.6 Solenoidal Winding Transformer Design -1 and Design -2 Design Result

7.6.1 Specification of Model-1 and Model-2 Design Result

	Design-1	Design-2
Type	Solenoidal separate winding	Solenoidal layered winding
Core material	Amorphous Alloy AMCC1000	Amorphous Alloy AMCC1000
Bac [T]	0.23	0.39
Core type	C-Core, AMCC1000	C-Core, AMCC1000
The number of cores	3pairs	3 pairs
Cross section area	72.15 cm^2	72.15 cm^2
Window area	42 cm^2	42 cm^2
Ap [cm^4]	3030	3030
Core volume [cm^3]	4522	4522
Core mass [Kg]	21.33	21.33
Number of primary turns	190	113
Number of secondary turns	20	12
Primary winding	19/29	19/29
Secondary winding	60/27	60/27
FEP insulation	0.0635cm	0.0635cm
Primary OD [cm]	0.271	0.271
Secondary OD [cm]	0.489	0.489
Thickness of airgap [mm]	0.025 (each side)	0.5 (each side)

Table 19 Comparison table

	Design-1	Design-2
Core loss [W]	56.45	141.50
Winding loss [W]	32.66	18.21
Total loss [W]	89.11	141.50
Self inductance	354.09mH	318.3mH
Coupling coefficient	0.9306	0.9975
Magnetizing inductance	329.52mH	317.5mH
Leakage inductance	49.15mH	1.60mH

Table 20 Loss comparison between 2 pairs and 3 pairs application

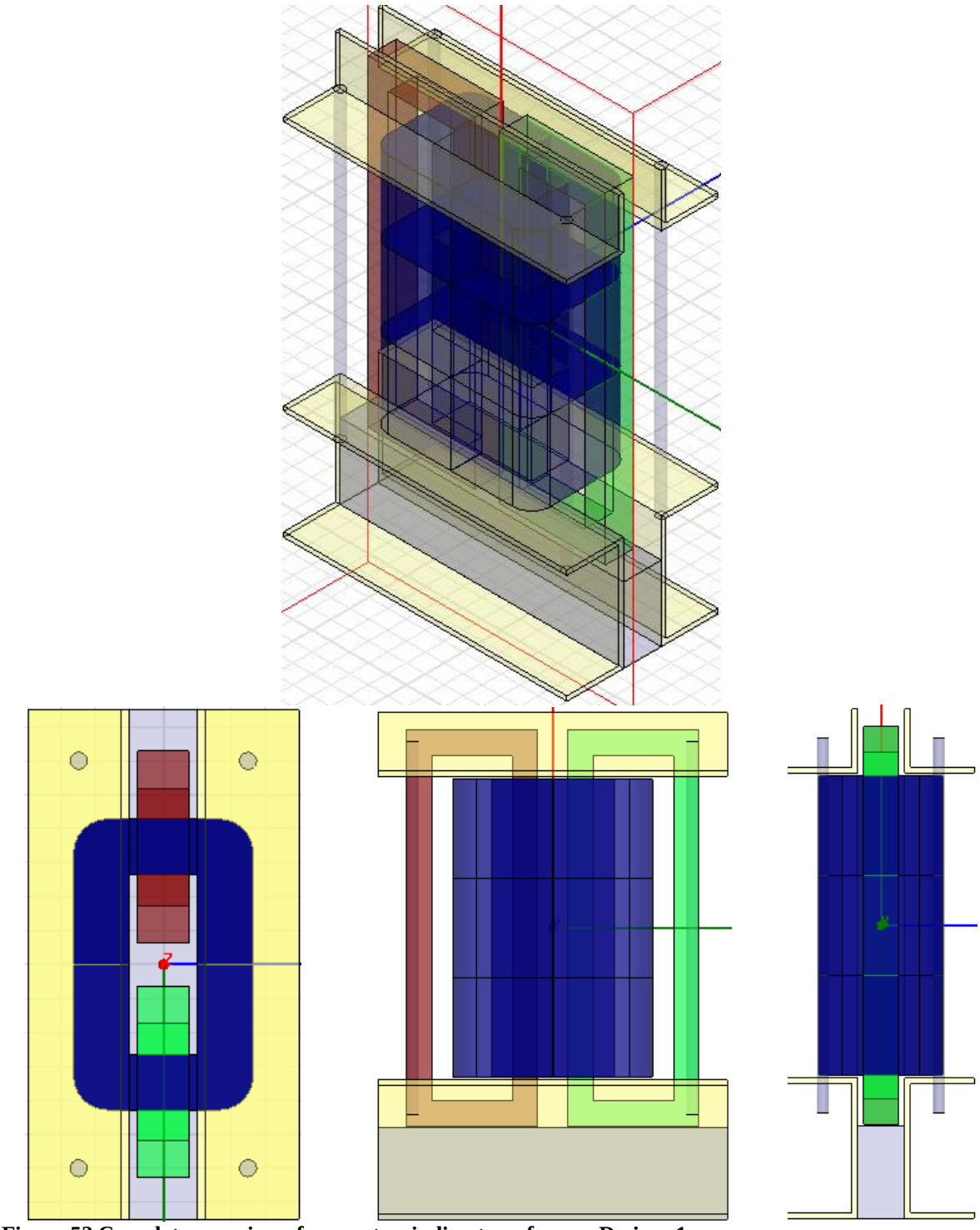

Figure 52 Complete overview of separate winding transformer Design -1

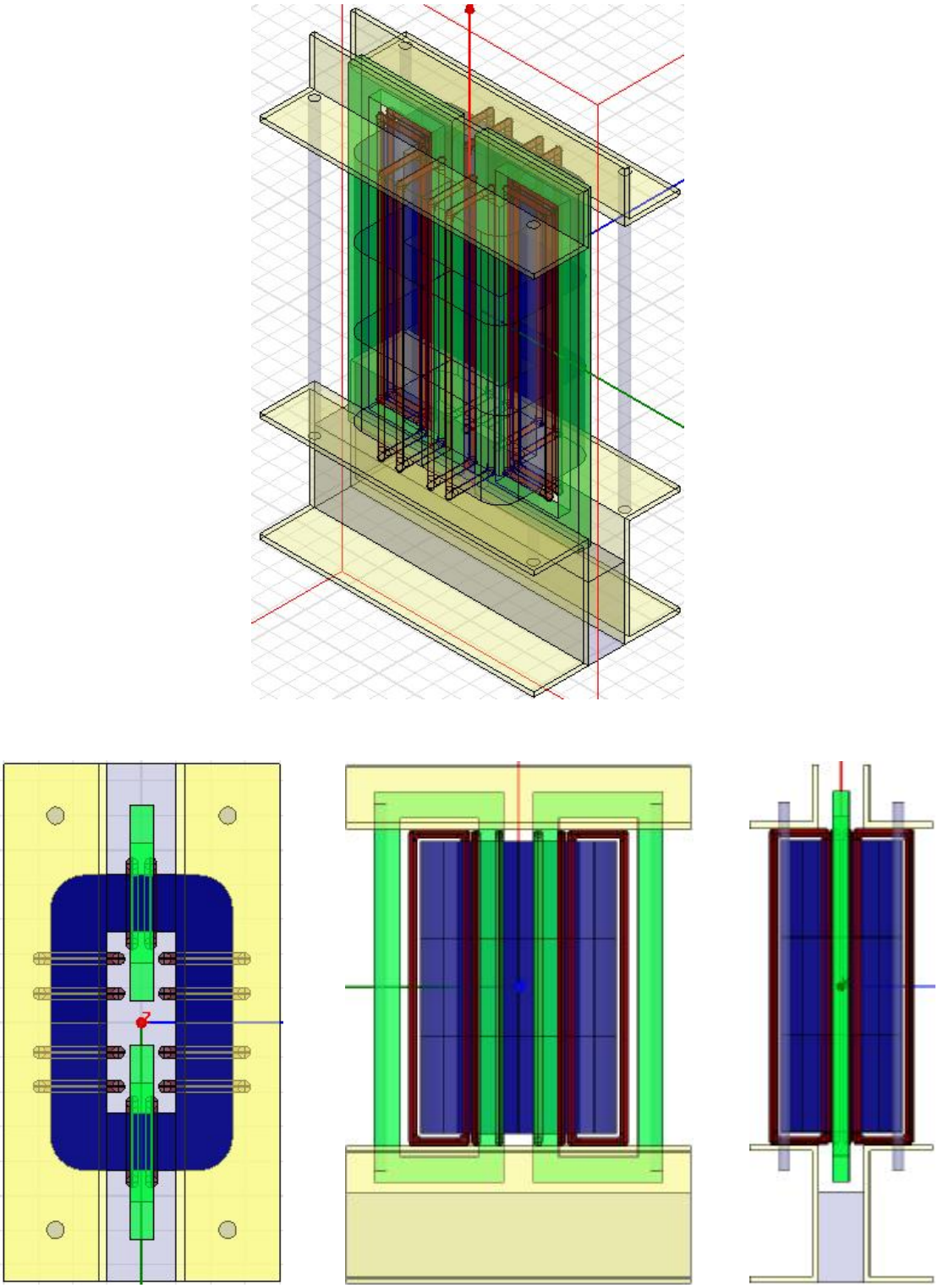

Figure 53 Complete overview of layered winding transformer Design-2

7.7 Coaxial Winding Transformer Model-3 Design Result

In case of coaxial winding transformer, single-turn outer winding is preferable because it is easier to build physically and the electromagnetic field can be predicted with more accuracy. Nonetheless, the SST application operates at high voltage and low current so that multi-turn of outer winding is unavoidable unless the advantage of small size in high frequency is given up. There are typically two ways to implement multi-turn outer winding for coaxial winding transformer, concentric tubes and split tubes. Concentric tubes has lower resistance than split tubes do due to larger cross section of copper area, but more complicated calculations are required and there is almost no advantage of copper loss under low current application such as Gen-1 SST high-frequency transformer. Therefore, split tube type outer winding must be better choice for this application. The 4 turns of outer winding and 38 turns of inner winding are required for SST application.

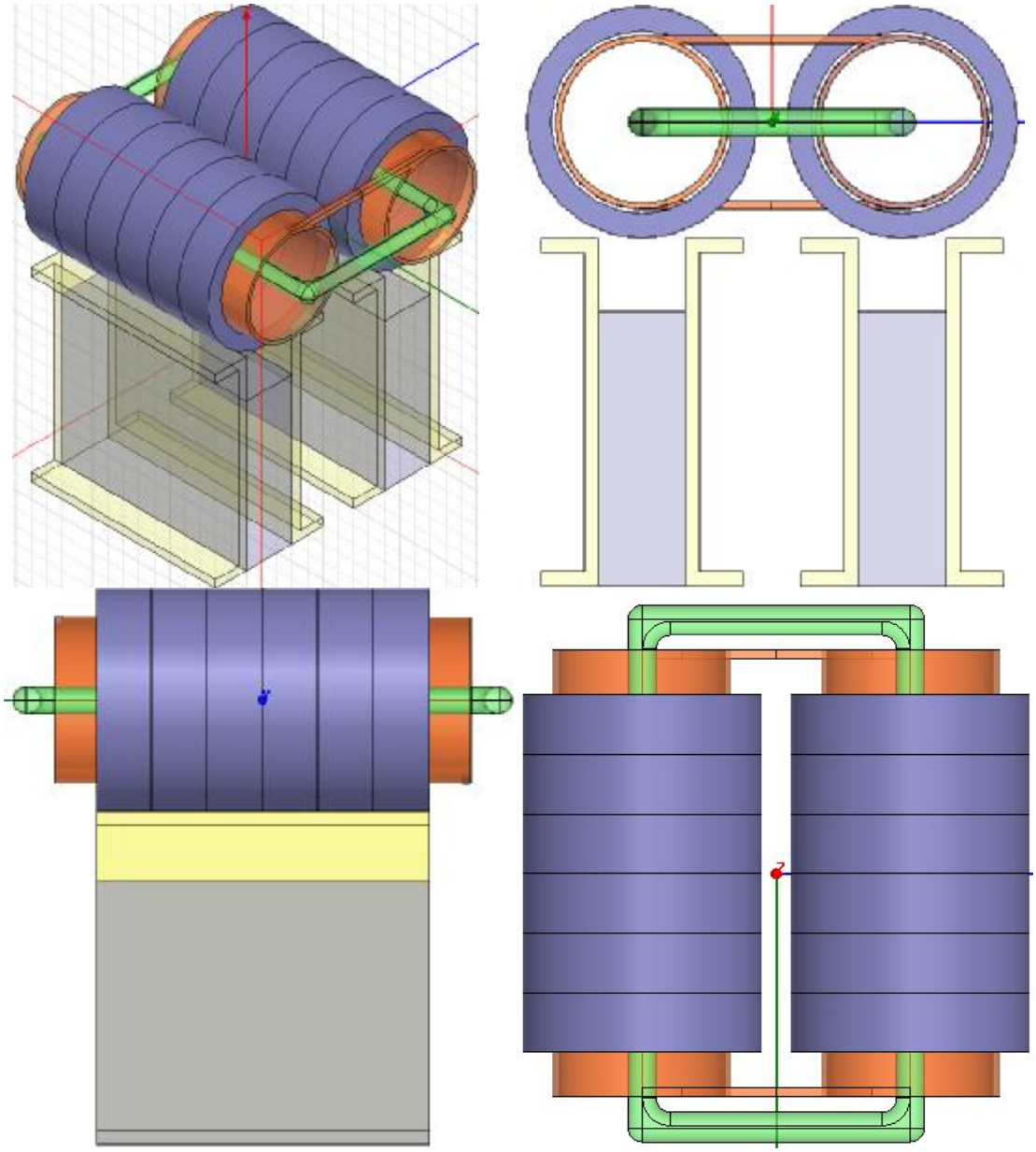

Figure 54 Complete overview of coaxial winding transformer Design -3

CHAPTER 8

8 EXPERIMENT RESUTL

In this experiment, substitute model which is scale-downed and simplified is used before original model is built and tested. First of all, actual permeability is required to measured and calculated to have a reliable value for more accurate simulation result The other important quantities to measure is magnetizing, leakage inductance and the other auxiliary parameters which will be compared to the simulation. As we discussed previously in the section which has calculation and simulation analysis, the same process is conducted to obtain magnetizing, leakage and other auxiliary parameters.

8.1 Specification of scale-down transformer

The power capacity of the transformer is reduced to approximately 2kVA with DC voltage of 400V and 5A on the both sides with 1:1 turns ratio. AMCC250 is chosen for this scale-down model based on the same process in which we have discussed in previous chapters and AWG15 with thin PVC insulation is used for wire on both sides. The geometry and the picture of real scale-down model is Fig. 55.

	High Voltage Side	**Low Voltage Side**
DC-bus [V]	400	400
Current at maximal load [A]	5	5
Power [W]	2kW	2kW
Turns ratio	1:1	
Switching frequency	3khz	

Table 21 Specification of transformer

Core Dimension [mm]						Performance parameters				
a	b	c	d	e	f	Lm[cm]	Ac[cm^2]	Wa[cm^2]	Ap[cm^4]	Mass[g]
19.0	25.0	90.0	60.0	63.0	128.0	31.4	9.3	22.5	210.3	2095

Table 22 Dimension of AMCC250 Powerlite C-Cores

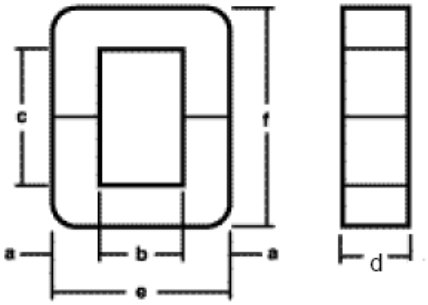

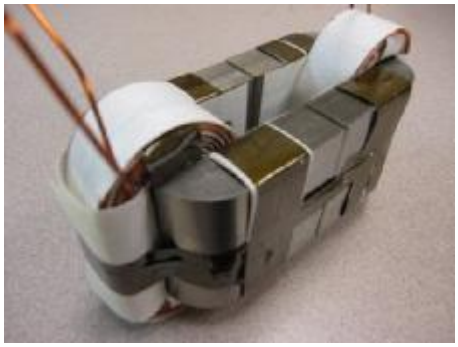

Figure 55 Core geometry(left) and real model

Gauge	AWG15
Diameter [mm]	1.45
Cross sectional area [mm^2]	1.65
DC resistance [$u\Omega / cm$]	104.5
Current density [A / cm^2]	303.03
Diameter of an equivalent square wire [mm]	1.285
The number of turns	78
The number of turns on each layer	13
The number of layer	6
Thickness of winding [mm]	7.71

Table 23 Specification of winding

8.2 Actual Permeability Measurement

We can obtain the actual permeability of the AMCC250 by the Ea() The calculated values over airgap thickness of 0.4mm are ignored because the permeability of core can be highly distorted with slight error due to the low contribution of permeability of core to inductance. The leakage inductance for this calculation does not have much impact and it is not reliably accurate at this point, so it is not taken into account and the errors can be corrected by a trial-and-error process. Hence, the final value of actual relative permeability of AMCC core made of amorphous alloy is 950.

$$L_M = \frac{n_1^2}{\frac{l_c}{m \cdot A_c} + \frac{l_g}{m_0 \cdot A_c}} \tag{8.2.1}$$

8.3 Magnetizing and leakage inductance of transformer with separate winding

The magnetizing and leakage inductance was measured with two different types of winding. The primary and secondary winding is totally separated and nomex paper as insulation material is placed between core and winding and layers.

The most crucial factor which forced to change the design of transformer was the permeability on datasheet is much differ rent from the values measured by experiment. The real permeability is calculated by simplified formula with data achieved from measurement and the real value is much lower than the one on datasheet, so the lack of magnetizing inductance becomes issues.

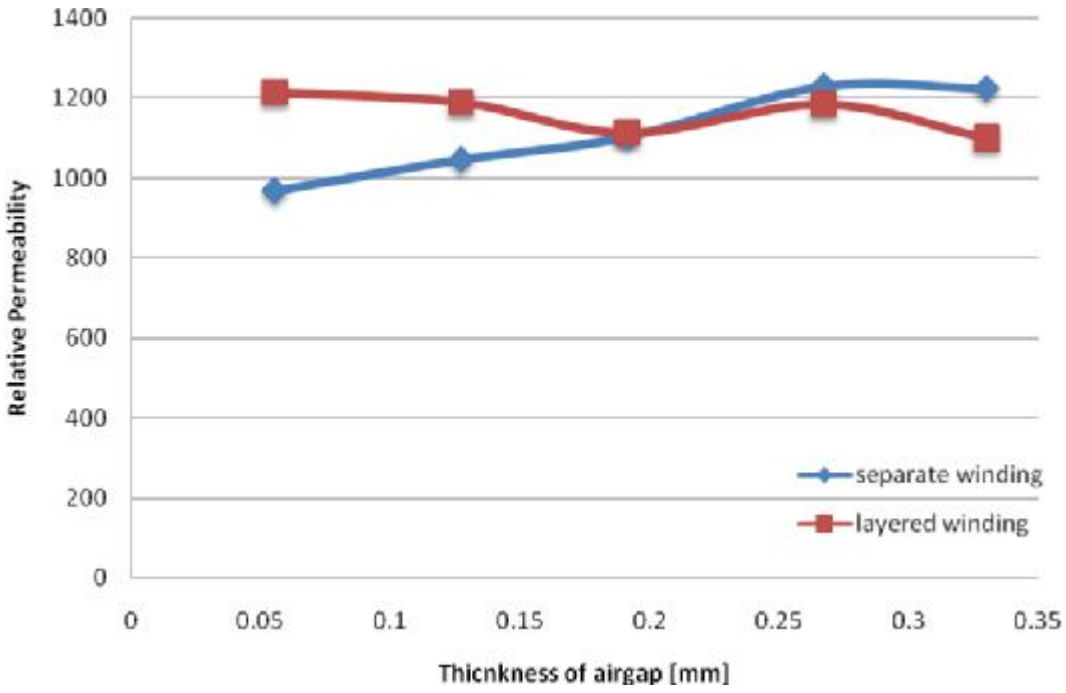

Figure 56 Experiment result of permeability of 2605SA1

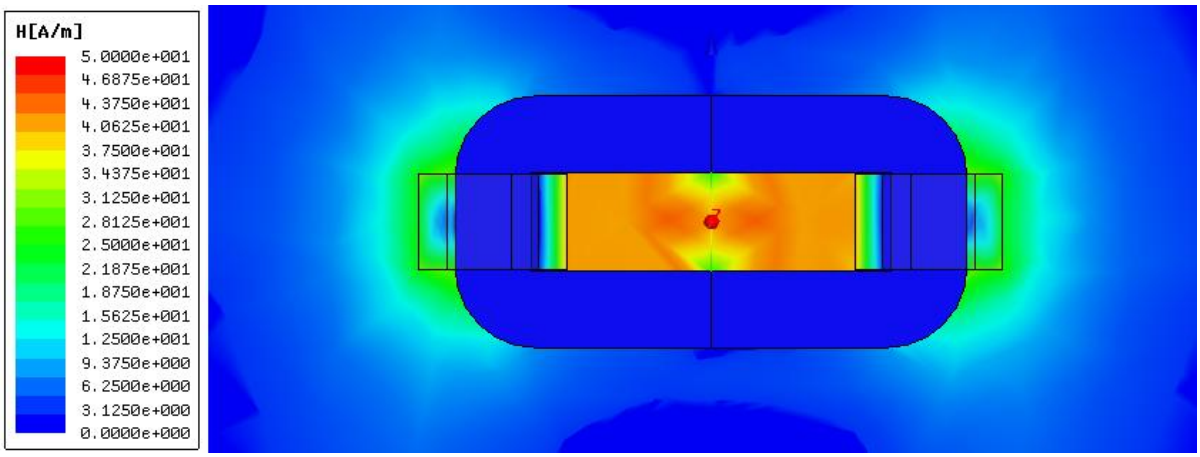

Figure 57 Magnetic field intensity distribution of scale-down transformer with separate winding

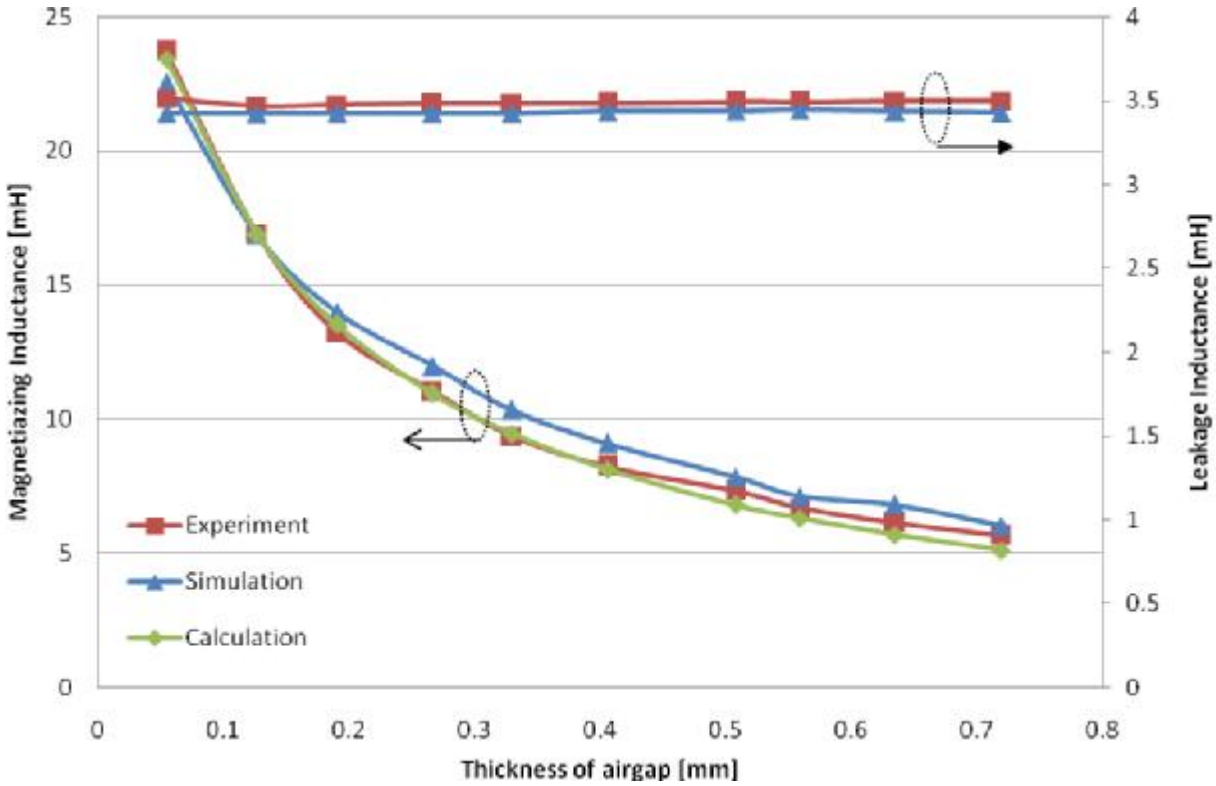

Figure 58 Comparison of magnetizing and leakage inductance between experiment, simulation and calculation with separate winding

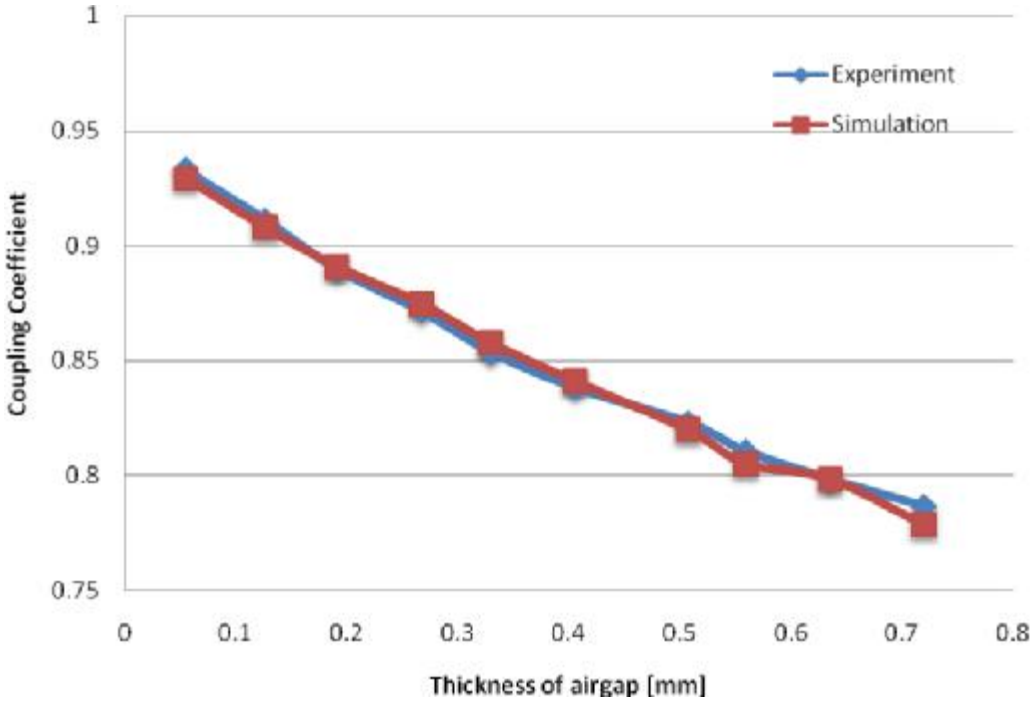

Figure 59 Comparison of coupling coefficient between experiment and simulation with separate winding

8.4 Magnetizing and leakage inductance of transformer with layered winding

Primary and secondary winding is split on both sides with the same number of turns. The primary turns are located at the bottom and 9mm thickness of paper is placed between both windings.

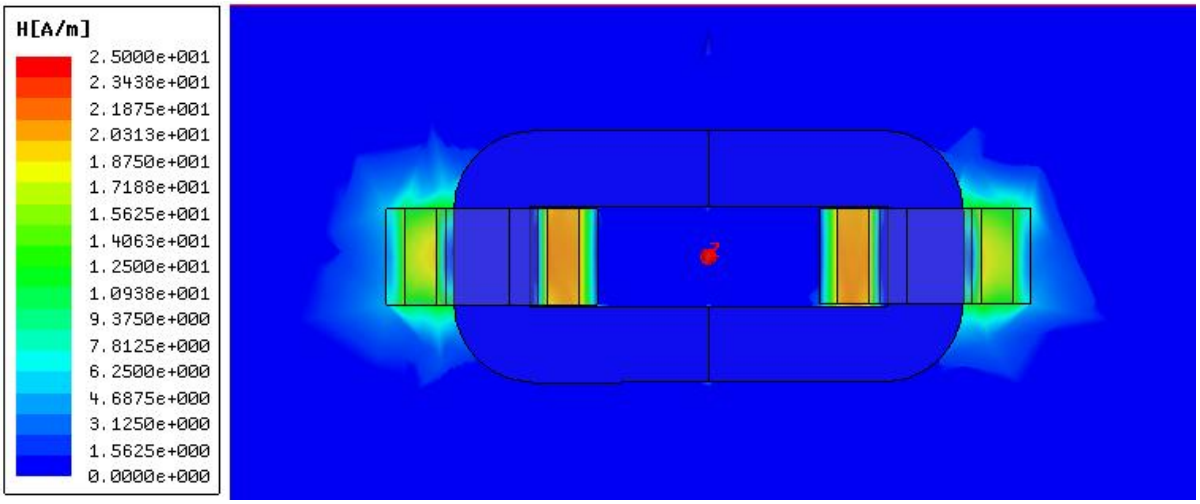

Figure 60 Magnetic field intensity distribution of scale-down transformer with layered winding

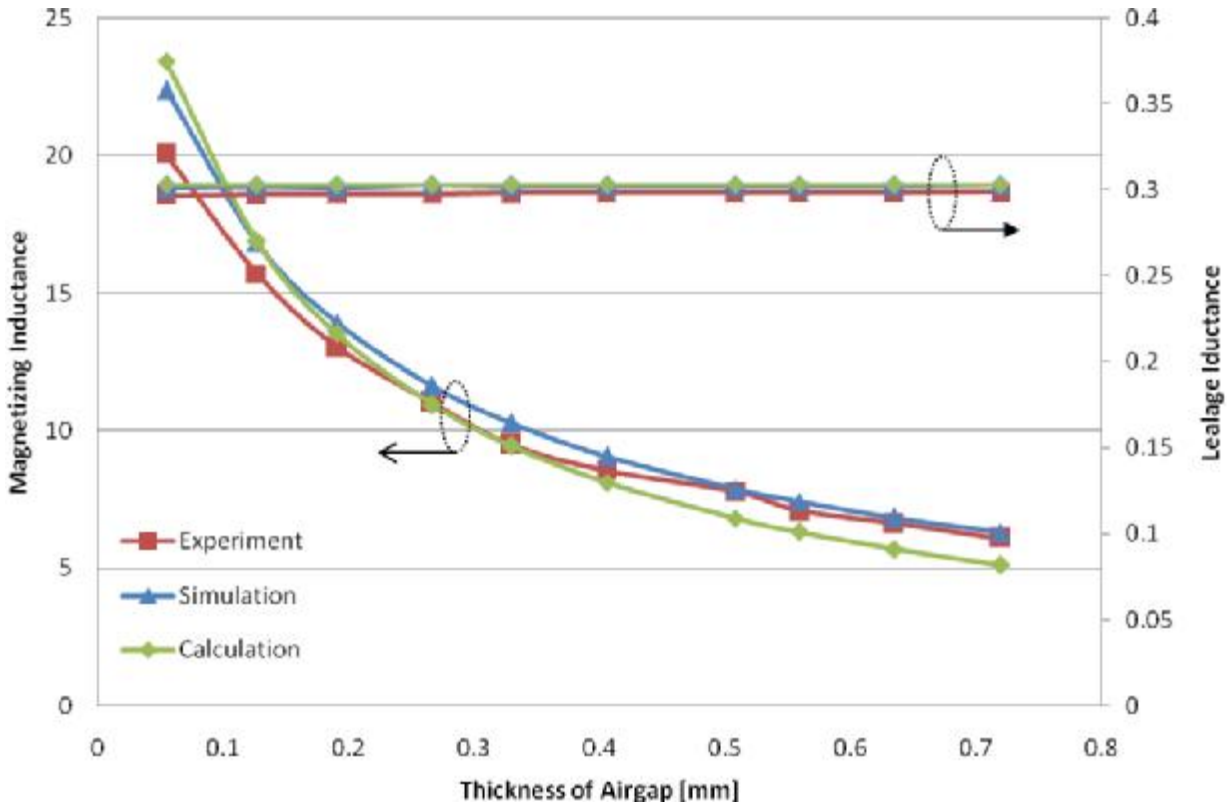

Figure 61 Comparison of magnetizing and leakage inductance between experiment, simulation and calculation with layered winding

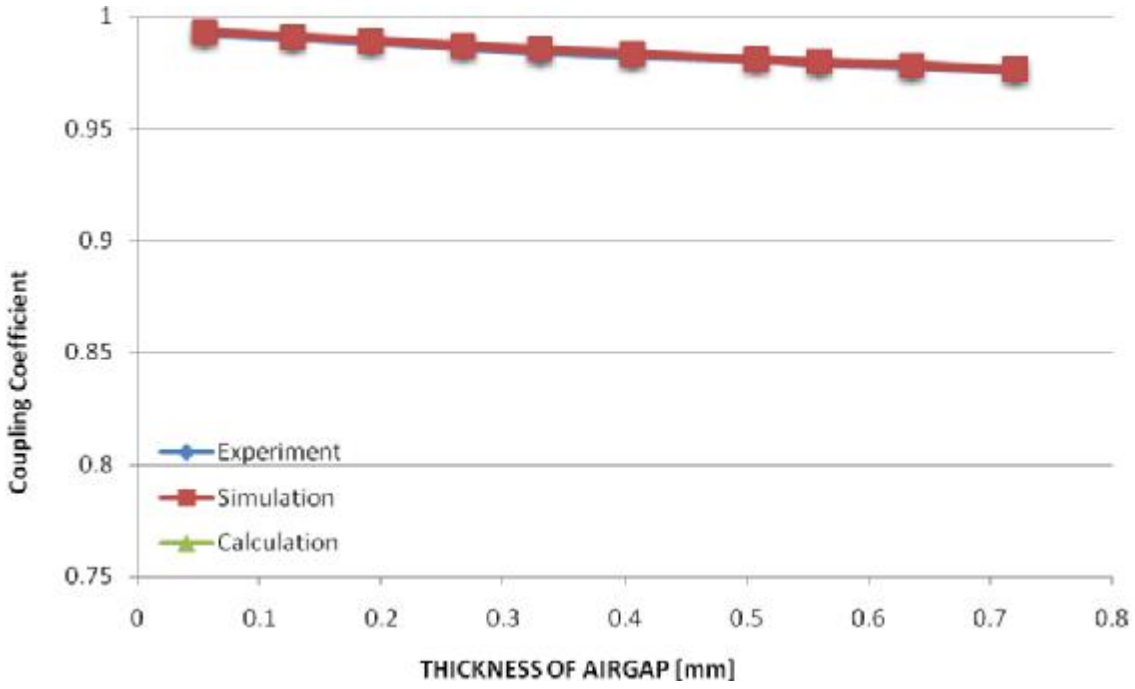

Figure 62 Comparison of coupling coefficient between experiment and simulation with layered winding

Line inductance Ls	1mH
Primary DC Capacitor	900uF
Primary DC voltage reference	400V
Secondary DC Capacitor	900uF
Secondary DC voltage reference	400V
Transformer turns ratio	1:1
Transformer magnetizing inductance	27mH
Transformer leakage inductance	3mH
DAB Switching frequency	5kHz
DC load	200Ohm

Table 24 SST prototype parameters

The prototype is implemented by using 600V 75A Intelligent Power Modules (IPM) based Si-IGBTs. The input is 240V AC voltage, the DC bus is 400V. A 1:1 high frequency transformer is designed for the dual active bridge stage. The SST control algorithm is programmed in DSP TMS320F28335.

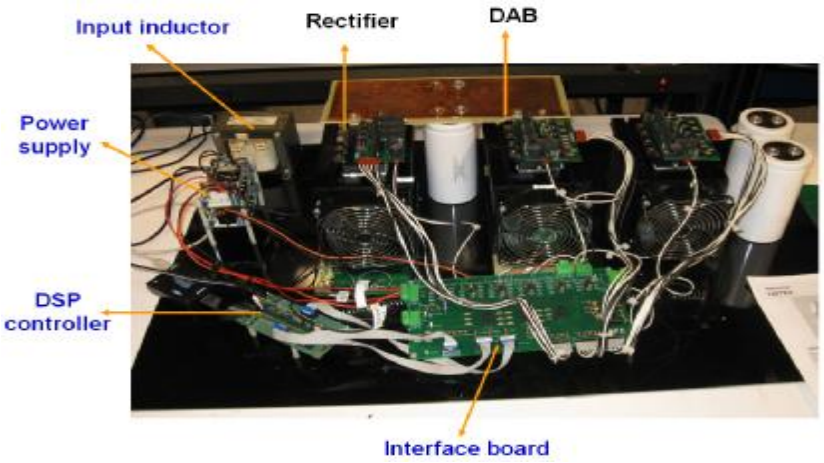

Figure 63 SST Prototype

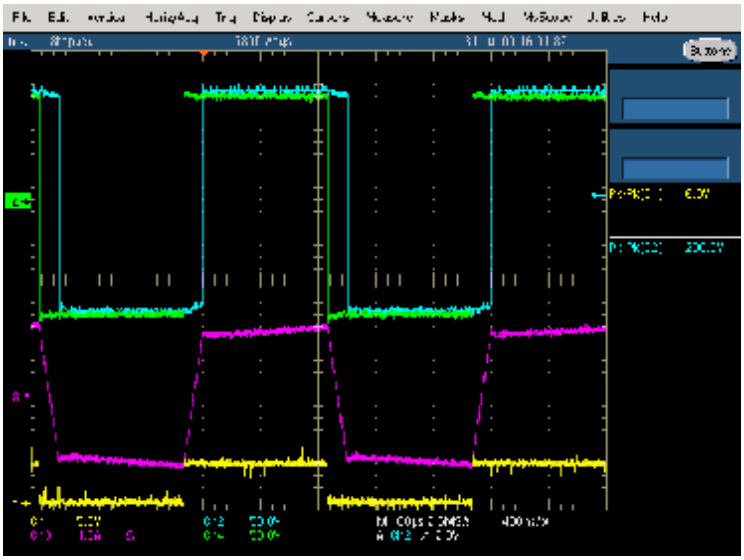

Figure 64 Waveforms of DAB converter with scale-down transformer

Ch1 Primary DAB gating signal, Ch2 Primary DAB voltage, Ch3 Primary DAB current, Ch4 Secondary DAB voltage

CHAPTER 9

9 CONCLUSION

Design -1 separate winding and Design -2 layered winding transformer are designed based on the same geometry and components except the method of winding. Basically, both of them have similar characteristics but the main difference between them is the amount of leakage flux and insulation concern.

First of all, Design-2 is designed by the most conventional design method. This method is relatively simple and feasible, however the high electric stress caused by 11.4 kV on the top stage has very high risk of electric breakdown and the small leakage inductance is rather a disadvantage for DAB converter application because additional inductors are required to meet the requirement to transfer rated power. The number of turns has to be necessarily reduced to have enough distance between parts to endure the high electric stress and the high flux density on cores due to the reduction of the number of turns which causes higher core loss and temperature rise as well. There is a slight advantage of winding losses as a result of lower number of turns but it is very small value considering the current rating of the SST is very small. On the other side, there is no electric stress between cores so no additional insulation is required between cores and the magnetizing inductance is very flexible due to no limitation of airgap thickness. This method could be good starting point to build transformer because of the relatively simple implementation.

The key point of Design-1 transformer design is eliminating the external inductor by adjusting leakage flux in itself. The external inductor required additional space, structure and cost as well. In contrast to the fact that low leakage inductance is typically preferable for traditional transformer design, this is a noticeable difference from the transformer design point of view. The leakage inductance is increased and adjusted by separating the windings on design-1 to eliminate the additional inductor. Nonetheless, the number of turns is high to reach the high leakage inductance so we should be careful not to make the window are too packed to avoid electric break down, especially, electric stress around airgap with high electric potential difference requires additional insulation method. The electric stress between primary core and windings are successfully reduced by connecting the primary core to low voltage terminal of the DC link on each stage as one of the solution.

It is obvious that Design-3 coaxial winding transformer shows superior performance. The size can be minimized by high frequency and the power losses are also not an issue thanks to the excellent characteristics of the nanocrystallin material. The cylindrical shape is ideal without edge effect except the ends of the structure from the insulation point of view and the very low and predictable leakage inductance becomes significant advantage once the operating frequency are increased more than 20kHz. Actually, most restraints come from outside, such as the frequency capability of switching devices and the power loss at the DAB converter so this design must come with development of new devices. One possible contingency is that the permeability of coaxial transformer without airgap is very high, so

there is a possibility of core saturation in case the DAB generates DC components. This practical issue will have to be taken care of on future work by experimental verification.

In order to meet the unique requirements for the SST application, the high voltage and high frequency transformer has been designed and built. The experimental results with scale-down 2kVA transformer have already shown the validity and accuracy of the proposed design procedure. The solid state transformer with Design-1 7kVA transformer has also been built now and will be tested under real condition once the high voltage test environment is ready.

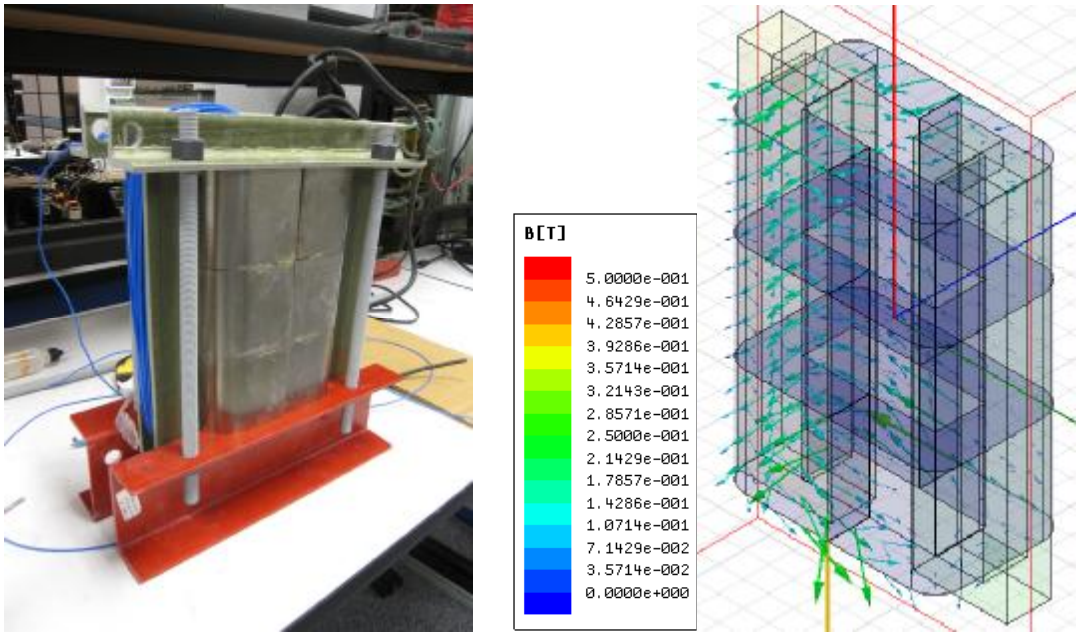

Figure 65 Design-1 7kVA separate winding transformer (left) and MAXWELL3D simulation result (right)

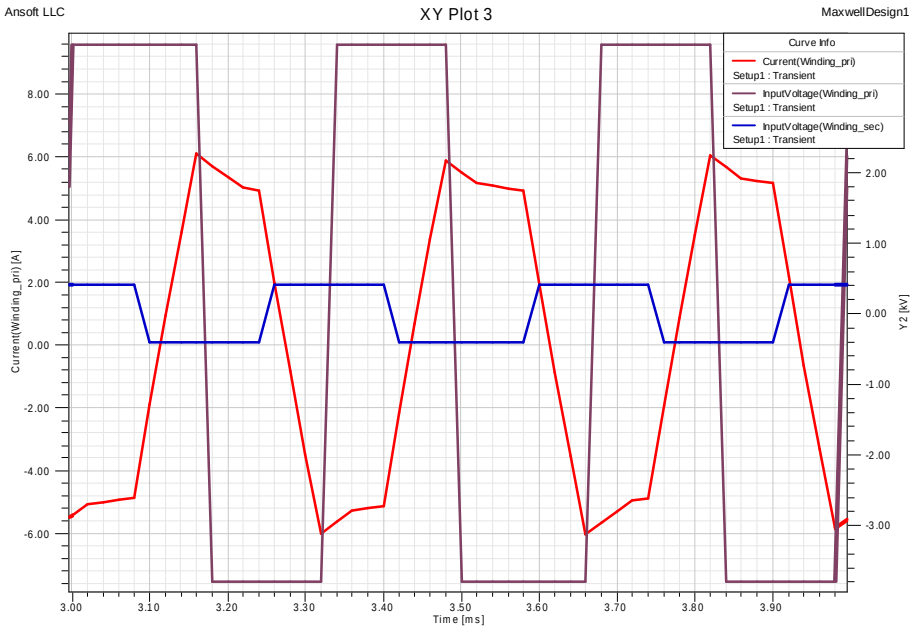

Figure 66 MAXWELL3D transient analysis with nonlinear B-H characteristics of amorphous alloy (primary current(red), primary voltage(brown), secondary voltage(blue))

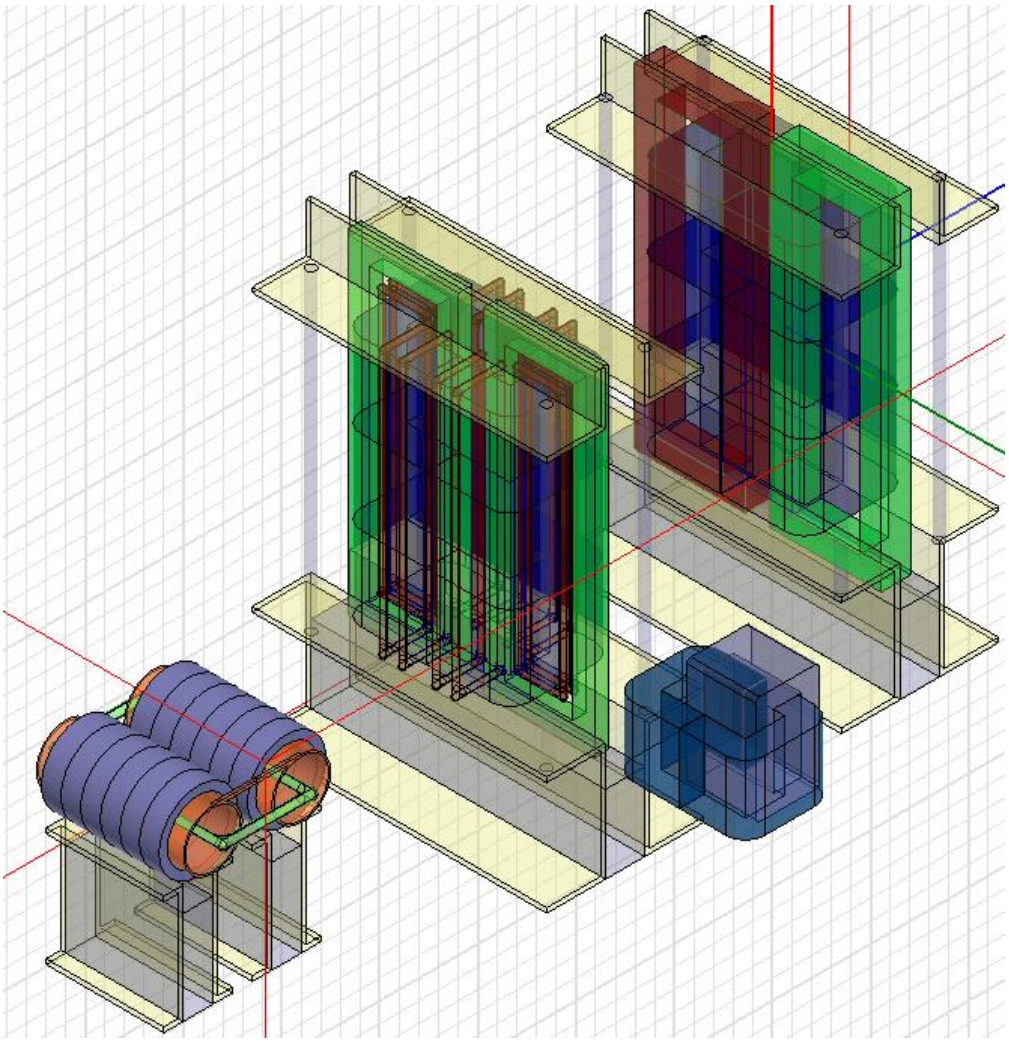

Figure 67 Overview of Models for size comparison

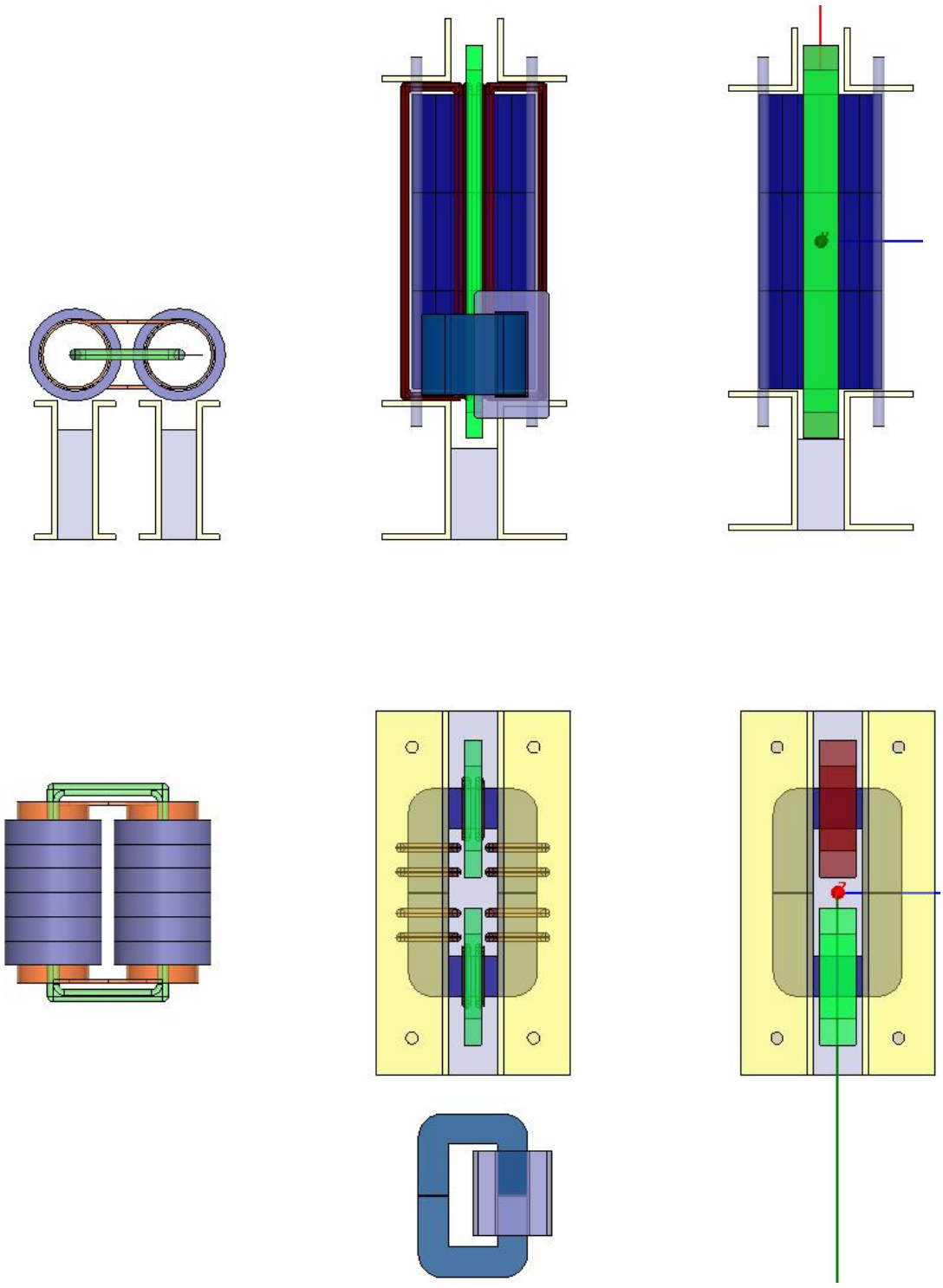

Figure 68 Top and Side view of Models for size comparison

	Design-1	Design-2	Design-3
Type	Solenoidal separate winding	Solenoidal layered winding	Coaxial winding
Core material	Amorphous Alloy AMCC1000	Amorphous Alloy AMCC1000	Nanocrystalline
Bac [T]	0.23	0.29	0.83
Core type	C-Core AMCC1000	C-Core AMCC1000	Toroidal Vitroperm 500
The number of cores	3 pairs	3 pairs	12
Cross section area	72.15 cm^2	72.15 cm^2	14.88 cm^2
Window area	42 cm^2	42 cm^2	31.17 cm^2
Ap [cm^4]	3030	3030	463.85
Core volume [cm^3]	4522	4522	1206
Core mass [Kg]	21.33	21.33	1.035
Number of primary turns	190	113	38
Number of secondary turns	20	12	4
Primary winding	19/29	19/29	19/29
Secondary winding	60/27	60/27	tubular copper
Primary OD [cm]	0.271	0.271	0.271
Secondary OD [cm]	0.489	0.489	N/A
Thickness of airgap [mm]	0.025 (each side)	0.5 (each side)	N/A
External inductor	N/A	AMCC1000	AMCC125

Table 25 Comparison table

	Design-1	Design-2	Design-3
Coupling coefficient	0.9306	0.9975	0.9994
Magnetizing inductance	329.52mH	317.5mH	317.74mH
Leakage inductance	49.15mH	1.60mH	0.53mH
Core loss [W]	56.45	141.50	46.17
Winding loss [W]	32.66	18.21	15.67
Total loss [W]	89.11	159.71	61.84

Table 26 Loss and inductance comparison between candidates

9.1 Future Work

1. Varnish-dip the 7kVA high frequency and high voltage transformer to prevent electric discharge and high voltage issues in cooperation with Waukesha Electric System.
2. Partial discharge high voltage insulation test at voltage 15kV in cooperation with Waukesha Electric System.
3. Take into account the possible high frequency characteristics of outer winding of Design-3 coaxial winding transformer
4. Combine the Design-1 7kVA high frequency and high voltage transformer into Gen-1 SST and test it under real condition.

REFERENCES

[1] Mustansir H. Kheraluwala, Donald W. Novotony, Deepakraj M. Divan, “Coaxially Wound Transformers for High-Power High-Frequency Applications”

[2] Mustansir H. Kheraluwala, Donald W. Novotny, Deepakraj M. Divan, “Coaxially wound transformers for High-Power High_frequency Applications”

[3] Mark S. Rauls, Donald W. Novotony, Deepakraj M. Divan, “Design Considerations for High-Frequency Coaxial Winding Power Transformers”

[4] Mark S. Rahuls, Conald W. Novotny, Deepakraj M Divan, Robert R Bacon, Randal W. Gascoigne, “Multiturn High-Frequency Coaxial Winding Power Transformers” IEEE transaction on industry application,vol VOL. 31 NO.1, Jan/Feb 1995

[5] Keith W. Klontz “Skin and Proximity Effect in Multi-layer Transformer Winding of Finite Thickness”

[6] Lloyd H. Dixon, Jr, “Eddy Current Losses in Transformer Windings and Circuit Wiring”

[7] S. N. Sen, A. K. Ghosh, “Variation of Townsend’s Second Coefficient in Electrodeless Discharge ”, PROC. PHSY SOC., 1962 VOL. 79

[8] O Coufal, “Current density in a long solitary tubular conductor”, IOP Publishing, Journal of Physics, 2008

[9] Linden W. Pierce, “Transformer Design and Application consideration for Nonsinusoidal Load Currents” IEEE transaction on industry application,vol NO.3, May/June 1996

[10] Mustansir H, Kheraluwala, Donald W. Novotny, Deepakraj M. Divan, “Coaxially Wound Transformers for High-Power High-Frequency Applications”, IEEE Transactions on power electronics, Vol 7, NO. 1, 1992,

[11] Mustansir H, Kheraluwala, Randal W. Gascoigne, Deepakraj M. Divan, Eric D. Baumann “Performance Characterization of a High-Power Dual Active Bridge dc to dc Converter”, IEEE Transactions on industry applications, Vol 28, NO. 6, 1992

[12] Keith W. Klontz “Skin and Proximity Effects in Multi-layer Transformer Windings of Finite Thickness”, IEEE

[13] Mark Rauls. “Analysis and Design of High Frequency Co-axial Winding Power Transformers”, Thesis for the degree for Masters of Science, 1992

[14] Mustansir H. Kheraluwla, “High Power High Frequency DC-to-DC Converters”, Thesis for the degree for Doctor of Philosophy, 1991

[15] Wei Shen, “Design of High Density Transformers for High Frequency High power Converter”, Thesis for the degree for Doctor of Philosophy, 2006

[16] McLyman, Colonel William T., “Transformer and inductor design handbook”, 1932

[17] M.S Naidu, V. Kamaraju, “High Voltage Engineering”, McGraw-Hill Professional, 1999

[18] Junming Zang, Fan Zhang, Xiaogao Xie, Dezhi Jiao, and Zhaoming Qian, “A Novel ZVS DC/DC Converter for High Power Application”, IEEE transactions on power electronics, Vol. 19, March 2004

[19] Ashkan Rahimi-Kian, Ali Keyhani, Jeffrey M. Powell, “Minimum Loss Design of a 100kHz Inductor with Litz Wire”, IEEE IAS Anuual meeting, Oct. 1997.

[20] Dr. Ray Ridley, High Frequency Power Transformer Measurement and Modeling”, Power system design Europe, 2007

[21]S. C. Kim, S. H. Nam, S.H. Kim, D. T. Kim and S. H. Jeong, “High Power Density, High Frequency, and High Voltage Pulse Transformer” IEEE, 2002

[22] K.Ferkal, M. Poloujadoff, E.Dorison, “Proximity Effect and Eddy Current Losses in Insulated Cables”, IEEE transactions on Power Delivery, Vol. 11, 1996

[23] Massimo Bartoli, Nicola Noferi, Alberto Reatti, “Modeling Litz-Wire Winding Losses in High-Frequency Power Inductors”, IEEE, 1996